AN INVESTIGATION OF THE ROLE OF INTERCRYSTALLINE BOUNDARIES ON THE DEFORMATION OF RECRYSTALLIZED ALPHA COPPER-ZINC

By
JACK EUGENE LEMONS

A DISSERTATION PRESENTED TO THE GRADUATE COUNCIL OF
THE UNIVERSITY OF FLORIDA
IN PARTIAL FULFILLMENT OF THE REQUIREMENTS FOR THE
DEGREE OF DOCTOR OF PHILOSOPHY

UNIVERSITY OF FLORIDA
1968

IN DEDICATION

TO MY WIFE

BENTA

ACKNOWLEDGMENTS

The author wishes to express his gratitude to Dr. F.N. Rhines. Without Dr. Rhines' patience, guidance, and encouragement this dissertation would not have been possible.

The author also wishes to express his appreciation to Drs. R.T. DeHoff and J.J. Hren, Professors of Metallurgy, Drs. J. Kronsbein and A.R. Quinton, Professors of Physics, and Dr. C.E. Reid, Professor of Chemistry, for serving on his supervisory committee.

The financial support of the National Aeronautics and Space Administration and the Department of Metallurgical and Materials Engineering is also gratefully acknowledged.

Finally, the author wishes to thank several members of the staff and student body of the Department of Metallurgical and Materials Engineering for their encouragement and assistance.

TABLE OF CONTENTS

TABLE OF CONTENTS (Continued)

LIST OF TABLES

LIST OF TABLES (Continued)

LIST OF FIGURES

LIST OF FIGURES (Continued)

LIST OF FIGURES (Continued)

LIST OF FIGURES (Continued)

LIST OF FIGURES (Continued)

LIST OF FIGURES (Continued)

Abstract of Dissertation Presented to the Graduate Council in Partial Fulfillment of the Requirements for the Degree of Doctor of Philosophy

AN INVESTIGATION OF THE ROLE OF INTERCRYSTALLINE BOUNDARIES ON THE DEFORMATION OF RECRYSTALLIZED ALPHA COPPER-ZINC

by

Jack Eugene Lemons

June, 1968

Chairman: Dr. F.N. Rhines
Department: Metallurgical and Materials Engineering

Brinell hardness was measured on bulk polycrystalline alloys of alpha brass as a function of grain size, alloy composition, and temperature. Brinell Hardness Number was found to be directly proportional to intercrystalline boundary area throughout the solubility range of alpha brass (0-35 w/o zinc) for the test temperatures of 77, 298, 573 and 873°K. The crystal boundary contribution to hardness maximizes sharply at 25 w/o zinc while the hardness of the crystal per se shows little sensitivity to composition. It is concluded that the intercrystalline boundary contribution to hardness resides in the structure sensitive transfer of plastic (but not elastic)

deformation from one crystal to the next through the intercrystalline boundary. At the 25 w/o zinc alloy composition of alpha brass, the relationship between hardness and structure is characterized by the fact that the stacking faults produced by crystal slip are at a maximum width. The energy otherwise required to pass shear through the crystal boundary is augmented by the energy required to close the stacking faults as they approach the intercrystalline boundary. At elevated temperature, similar behavior is encountered when high rates of deformation prevail; with normal rates of deformation the closure of stacking faults is aided by diffusion processes, which are rapid at high temperature and which decrease the energy necessary to pass shear through the intercrystalline boundary. The alpha solid solutions of the system silver-zinc displays similar behavior except that the stacking faults widths are narrower and the contribution of the intercrystalline boundary to the total hardness is likewise smaller.

CHAPTER I

INTRODUCTION

It was realized early in the history of metallurgy that metals have an internal structure and that the dimensions of this structure are important in determining the properties of the material. The development of superior mechanical properties through grain refinement has been practiced for a very long time and interest in the analysis of relationships between these parameters can be traced back to the early metallographers in the 18th century. Within the past fifty years or so, many attempts have been made to establish quantitive relationships between grain size and mechanical properties. These studies have been successful in showing the reality of the relationship but have not established any specific relation which can be generally applied to identify the mechanism by which grain size influences properties. Within recent years, quantitative metallography has undergone an extensive development which has made it possible for the first time to correlate mechanical properties with rigorously defined geometric

parameters. The time is therefore opportune to approach this subject with new and better tools with the intent of explaining the role of structure.

1.10 Grain Dimensions in Polycrystalline Aggregates

Réaumur (1722) was one of the earliest metallographers to employ a microscope in grain structure studies of polycrystalline metals. He examined fractured surfaces of steel and cast iron and suggested a polyhedral grain shape. While it has generally been found impractical to examine isolated grains, it is always possible to make a plane section through the aggregate and to examine the size and shape of grain sections on the plane of polish. The technique of studying microstructures on plane polished sections found its useful beginning with Sorby (1882) and coworkers in the late 1800's. The fine structure of metallic aggregates and the meaning of properties in terms of structure rapidly gained interest, but it was not until the presentations of work by Heyn (1903) and Jeffries (1916) in the early 1900's, that structure measurements were put on a semiquantitative basis. These measurements were immediately tested in their relation to mechanical properties hoping to

reveal fundamental and general laws. The ensuing investigations are too numerous for separate consideration, but in general, most failed because of incorrect interpretations of aggregate grain dimensions.

Desch (1919) was perhaps the first investigator to conduct an extensive study into the true three-dimensional form of aggregate grains. His investigations,which were later extended by Hull and Houk (1953), showed that although a two-dimensional section through a beta brass polycrystal gave supposedly regular and equiaxed grains, when the grains were separated by mercury penetration, no identical grains existed. These investigations attempted to define what polyhedron most closely approximates the average grain in a metal. The conclusion was that grain shapes are irregular and can not be completely characterized by any polyhedron.

Saltykov (1945) was the first to derive a relationship whereby the boundary area of interface per unit volume of aggregate (a rigorous geometric property) could be accurately determined by measurements on a two-dimensional section. Later investigators, Smith and Guttman (1953), Duffin, Meussner, and Rhines (1953), and Titel (1953), independently derived and introduced the same relationship, i.e., the

ratio, N_L, of the number of intersections made between a known length test line and grain boundary traces is an unbiased estimator of the grain boundary area per unit volume. The only restrictions are that test sections must be representative of the grain structure, and that a statistically meaningful sample be counted. The relationship is $S_v = 2N_L$, where S_v is the total area of interface per unit volume of structure. Smith and Guttman's (1953) paper is a classic presentation of the principles involved in true measurements of aggregate structure dimensions. They point out the fallacy in interpreting two-dimensional mean grain intercept as three-dimensional grain diameter, although more recent investigators either have not accepted or are not aware of these long-known principles.

Intercrystalline boundary area is the first polycrystalline aggregate structure measurement that has a clearly defined and physically interpretable meaning in its relationship to mechanical property measurements. Other geometric parameters, such as those introduced by Heyn (1903), Jeffries (1916), and other early investigators were attempts to approximate the three-dimensional properties without the awareness of true topological measurements and their meaning.

Determinations from a single plane section, such as the average path length between grain boundaries yield a sum in unit volume of the specific property that is measured. To obtain a three-dimensional measurement such as "grain diameter" it is necessary to divide the "sum" by the number of grains per unit volume. The number of grains per unit volume is not obtainable from a single plane section, and therefore the earlier measurements of "grain diameter" were not related to space properties, but rather to properties of the cross section. It so happens that most of the measurements that were incorrectly related to the "grain diameter" actually measure some function of intercrystalline boundary area.

A specific example of this can be found in the investigations of Petch (1953) and followers. In general, they have used either (1) a N_L type measurement directly, or (2) some function of the number of grains per unit area, to determine so called "grain diameters." Both of these measurements were made on two-dimensional sections without any knowledge of the number of grains per unit volume. Therefore, any correlations made with mechanical properties

does not relate to "grain diameter" as supposed but rather to some function of the intercrystalline boundary area.

1.20 Hardness

Historically, several types of hardness measurements have evolved simultaneously, with each specific test suited to the needs of the originator. This has resulted in several connotations for the word hardness. Broadly, hardness measurements fall into three categories: scratch, rebound, and indentation. Scratch hardness is the oldest having been first introduced by mineralogists. The most widely used scratch scale depends on the work of Mohs (1822) who used the mineral standards. The scale starts with talc (scratch hardness 1) and ends with diamond (scratch hardness 10). This scale, although useful to the mineralogists for the classification of minerals, is limited because of not being quantitative, nor directly related to other hardness numbers. Another example of a hardness scale that relates to specific material properties is the rebound measurement. For instance, the Shore (1913) rebound sceleroscope measures the rebound distance of a hard ball,

and for the most part is a measure of elastic properties. Indentation hardness, as it is most commonly measured, is simply the resistance of a material to plastic deformation. Common indentation tests can be grouped into three categories: (1) the Brinell, or Meyer, type measurement where a spherical indenter is pressed into the test material until the externally applied load is just balanced by the material's resistance to deformation; (2) the Rockwell type measurement where a balance is not necessary and the measurement depends upon a depth of timed penetration at a set load; and, (3) variations and combinations of (1) and (2). Within limits, indentation hardness scales are qualitatively interrelatable as a group, but in general the scales of scratch, rebound, and indentation are not interconvertible. This situation was pointed out by O'Neill (1934) when he wrote that hardness "like the storminess of the seas, is easily appreciated but not readily measured." Several advocates of hardness testing have written books on the practical, theoretical, and philosophical aspects of hardness. Two of these are O'Neill (1934) and Tabor (1951) and the reader is referred to them for a complete introduction to the general aspects of hardness and its measurements.

In this research, hardness tests were all of the indentation type where hardness numbers are expressed in the dimensions of pressure, i.e., equilibrium load per support area. There were several reasons for choosing indentation hardness as opposed to the other type of mechanical tests. For instance: (1) indentation hardness is a static type measurement that attempts to read a final result where plastic deformation has come to an end and the applied load is just balanced by the resistance of the subject material across the support surface, whereas other measurements such as the various yield strengths attempt to read either a predetermined point, or a slope along a dynamic load versus displacement diagram; (2) indentation hardness tests only require one relatively smooth and flat external surface while compression and tensile test specimens require an exact length and cross section geometry; (3) hardness measurements are non-destructive; (4) hardness is sensitive to grain size in polycrystalline aggregates; (5) hardness is the only test available where a single grain, several grains, or an aggregate's properties can be measured and compared within one polycrystalline specimen. For these reasons, indentation hardness has been used as a tool to study the mechanical properties of polycrystalline aggregates with respect to their dependence upon structure.

This does not mean that useful information could not be obtained from other types of measurements, but rather that indentation hardness is a superior measurement for this particular study.

It has long been known that the Brinell hardness of many metals increases as the grain size becomes finer. In the present research this effect has been verified repeatedly and it has been shown that the hardness is, in fact, proportional to the area of grain boundary. This response of Brinell hardness to grain size is, moreover, much more distinct and regular than the response of tensile or compressive yield strengths to grain size. This difference is perhaps associated with the well established fact that the Brinell Hardness Number is a load per support area which balances the sum of two resistances to deformation, one being the fundamental elastic resistance of the material in its pretest condition, the other being the added elastic resistance provided by strain hardening, whereas the yield strength (ideally) senses the fundamental elastic resistance alone. A careful analysis shows that the major part, possibly all, of the grain size sensitivity to Brinell hardness is to be associated with its resistance

to plastic deformation per se. In other words, it appears that the plastic response of a metal is sensitive to grain size, whereas its true elastic response feels only the crystalline properties, irrespective of crystal boundaries.

Justification for the separation of the initial elastic resistance (without prestrain) and the added resistance provided by plastic deformation, and their separate relation to structure is obtained by comparing the investigations of Harris (1922) and Lemons (1964). Harris (1922) managed, through unique testing techniques, to exclude strain hardening contributions from Brinell hardness measurements on alloys of alpha brass. By eliminating strain hardening, this hardness number measures the equilibrium load that is just balanced by the resistance of an elastically (but not plastically) strained subject material across a support surface, and comes as close to measuring an elastic limit as is possible with an indentation hardness test. In all cases, Harris's (1922) strainless Brinell hardness measurements are lower than normal Brinell measurements. This shows that the normal Brinell number is composed of both an elastic and plastic material contribution. To consider the role of structure per se, it is

necessary to include the work of Lemons(1964), who made Brinell measurements on alpha brass alloys, studying the effects of grain size. As previously mentioned, Lemons' (1964) experiments showed that Brinell hardness was directly proportional to intercrystalline boundary area. This direct proportionality provided a method for the separation of the hardness contribution of an average aggregate grain[1] from the gross measurement of grains and grain boundaries obtained from a polycrystalline hardness number. A comparison of the average grain, polycrystalline, and strainless hardness measurements shows that the strainless hardness is lower than the average grain hardness by a constant value, while the magnitude of the polycrystalline hardness depends upon intercrystalline boundary area. Thus, the magnitude of the polycrystalline Brinell hardness must be associated with an interaction between structure and plastic deformation. Therefore, the Brinell or similar indentation hardness tests are seen to be ideally suited to the measurement of structure sensitivity to plastic deformation, and have been used exclusively in the research that will be described in this text.

---

[1]Average grain means an average with respect to crystallographic orientation.

Apropos of indentation hardness measurements, a historical introduction to the specific test used in this investigation is in order. These tests and their relation to material properties will be considered in two distinct but related categories: (1) macrohardness, where large indenters and loads are used to test average grain and grain boundary properties, and (2) microhardness where small indenters and loads are used to test the properties of local or separate features such as grain centers or grain boundaries. Names associated with these tests are: (1) Brinell macrohardness, (2) Meyer macrohardness, and (3) Vickers microhardness.

Almost since its beginning, the Brinell Hardness Number has been a commonplace designation in material specifications. Brinell's thoughts expressed during the development of the test might help to provide insight into the reasons for this general acceptance. J.A. Brinell was chief technical manager at the Fagersta iron and steel works in Westmanland, Sweden during the formative era of his hardness test. He wanted a ready, easy, and at the same time, trustworthy means for controlling what was then

called the "forging tests." These "forging tests" give the relative hardness of materials. Brinell decided to use a ball for hardness testing because of availability and the thought that a spherical indenter would give more consistent results in a variety of places. The mechanics of the test consisted of placing a ball bearing on the test material and applying a known load to the upper side of the ball. The test was complete when the ball came to rest and remained essentially static with the load applied.

Brinell set up these criteria for a hardness test: (1) it must give trustworthy results, (2) it must be easy to learn and apply, (3) there should be no need for costly or time wasting mechanical treatment of the materials previous to testing, (4) the indenter should be cheap, easy to obtain, incapable of changing its shape, and of a sufficient hardness, (5) the method should be applicable to finished articles, as for instance, armor plates, projectiles, and the like, and (6) the testing results should be indicative of the absolute hardness of the material tested. The Brinell Hardness Number (BHN) proposed by Brinell used the load applied to the ball divided by the

curved surface area made during the impression. Standard units are kilograms per square millimeter.

The question often arises, why did Brinell use the curved impression surface area rather than the projected surface area? Wahlberg (1901) in his account of Brinell's investigations and thoughts, says without explanation, that the curved area tends to compensate for strain hardening. Some sense of the reasonableness of this assertion may be derived from the fact that the rate of change of curved area is more rapid than the projected area and would have the effect of decreasing the hardness number for deep impressions. In other words the meaning of the test becomes ambiguous when the test impression diameter approaches the diameter of the indenter. In the current investigations, hardness numbers determined from curved area were within 1 per cent of those determined from projected area in all cases.

Meyer (1908) discovered a method whereby a Brinell type hardness test could be extended to the separate evaluation of both the pretest hardness and the rate at which the material under the ball hardens during the test. Both of these measurements are obtained from an empirical

relationship between the applied load and the hardness impression diameter.

Meyer (1908) found for twenty-eight different metals that the load applied to a constant size ball was related to the impression diameter through the equation $L = kd^n$, where L = load in kilograms, d = chordal diameter of the impression in millimeters, k = load in kilograms when d equals 1 millimeter, and n = coefficient relating to the strain hardenability. The pretest hardness number is different from a normal hardness number because the impression size is constant (d= 1 millimeter) and the load (k) varies. Therefore the pretest hardness number is proportional to k because of the constant support area. It was called "pretest" because it relates to a very early stage of the deformation process where supposedly very little strain hardening of the material under the ball had taken place. The strain hardening coefficient (n) does not measure a hardness per se, but rather a rate of hardening during the indentation process. Therefore it can not be obtained from a single hardness test, but requires a series of tests to establish the relationship between load and impression diameter. The coefficient

(n) can be used as a measurement of: (1) the rate of strain hardening during the test, or (2) the amount of strain that was already present in the material before the test started. For instance, most recrystallized metals have a coefficient of about 2.5 (they strain rapidly during the test, but contain no prestrain) while worked materials approach a limiting coefficient value of about 2.0 with increasing work content (they strain harden very little during the test, but contain large amounts of prestrain). Meyer's (1908) analysis, although empirical, is found to hold over a wide variety of materials and conditions including the specific materials currently studied by the writer. Therefore, both pretest and strain hardening will be investigated in this research.

Meyer Hardness Number (load per square millimeter of projected area) is generally preferred over Brinell Hardness Number (load per square millimeter of curved area) because Meyer hardness is interpretable in terms of an average pressure measurement. A comparison of Meyer and Brinell hardness is given with the average pressure derivation in Appendix I. Throughout this investigation, both

hardness measurements are acceptable in that they are not different by more than 1 per cent. Since Brinell hardness is most widely known, it will be used in subsequent chapters except when comparisons are made with compression and tension type stress versus strain investigations.

The microhardness test, known by the name of Vickers, is the product of an evolution through many different types of hardness measurements. The "Father of Micro-Indentation Testing" was Le Gris (1911) who used the end of a glass rod formed into a spherical tip micro-indenter to measure the relative hardness values of phases in two phase alloys. Although a start, the microhardness technique of Le Gris (1911) was unhandy and very limited in general application. For instance, the micro-indenter was both fragile and small, and the resulting impression diameters could not be accurately measured without a microscope. A major improvement was made a few years later when Lips and Sack (1937) mounted a micro-indenter interchangeably with a microscope objective. The result was that microhardness measurements were greatly facilitated and in fact, made practical by indenting and measuring

on a single instrument. These original ideas have carried over, and within the past few years the range and accuracy of the microhardness test has been greatly extended. Currently available microhardness testing machines are equipped with a variety of optical measuring devices, indenters, loads, and loading rates.

The major applications of microhardness measurements depends upon their size. These small impressions and the resulting zone of plastic deformation can be limited to a local region. They are therefore useful in the comparison of constituents or structure within a single specimen. In general, this is the application made of microhardness in this research where low load measurements are used for: (1) relative comparisons of grain center and grain boundary regions, (2) studying average grain center microhardness as a function of alloy composition, and (3) comparisons with previous microhardness investigations on similar test materials.

1.30 Hardness as a Function of Grain Dimensions

Many attempts have been made to determine the influence of grain boundaries on the mechanical properties

of polycrystalline metals. The literature pertaining to the current investigation is so voluminous that the writer finds it necessary to limit his survey of it to a specific subject area. The literature survey that follows deals with the grain size-hardness relationships in copper and alpha brass, where the grain size has been measured and expressed in explicit terms.

Bassett and Davis (1919) studied the effects of grain size on the Brinell hardness of 68-32 copper-zinc. Grain dimensions were approximated by a so called "grain diameter (d)" which was determined from Jeffries (1916) formula $d = (n)^{-1/2}$ where n is the number of grains per unit area. The range of "grain diameter" investigated was from 0.024 to 0.353 millimeters. Hardness increased at a non-uniform rate with decreasing "grain diameter," showing the largest increase below 0.05 millimeters. Norbury (1923), upon noting the results of Bassett and Davis (1919), decided to conduct a similar investigation on pure copper. Early in his investigation, it became apparent that the Brinell hardness of copper was relatively insensitive to grain size. Angus and Summers (1925) introduced the expression $3(n)^{1/2}$ which they call "grain

boundary area." This was derived on the assumption that grains can be approximated by cubes. The term n is the number of cubes per unit area (assumed to be the number of grains per square millimeter). Data on several materials including copper and cartridge brass (70-30 copper-zinc) showed that the relation between $3(n)^{1/2}$ and hardness approximated a straight line. The concept of grain boundary area and its relation to hardness measurements remained relatively dormant for the next few years until Babyak and Rhines (1960) revived the concept using a clearly defined relationship of quantitative metallography. Their investigation showed that the Brinell hardness of polycrystalline cartridge brass was directly proportional to accurately determined grain plus twin boundary area. The boundary area was statistically determined through N_L measurements and showed that the scatter associated with previous approximate relationships was eliminated. This research was the first investigation to express the grain dimensions in mathematically definable terms, although in the written discussion by other investigators, the concept was criticised on the lack of fundamental interpretation.

This same type of investigation was continued by the writer in 1962 on copper, 90-10 and 70-30 copper-zinc. Brinell hardness was found to be directly proportional to intercrystalline boundary area at all of these compositions. A comparison of the 70-30 copper-zinc data with the previous investigation of Babyak and Rhines (1960) showed the two relationships between boundary area and hardness to be identical. This result was stimulating because alloy heats and specimen production procedures were different in the two cases. Further comparisons of similar properties, such as hardness at a predetermined value of boundary area, showed a strong compositional dependence, e.g., cartridge brass of a fine grain size was two times harder than copper of comparable grain size, with commercial brass (90-10 copper-zinc) falling in between. The writer was encouraged by this result to undertake an examination of the effect of the zinc content upon the hardness-intercrystalline boundary area relationship in alpha brass.

Lemons (1964) measured Brinell hardness as a function at intercrystalline boundary area for seven alloys spanning the complete solubility of alpha brass. All

measurements were made at room temperature following the basic experimental techniques introduced by Babyak and Rhines (1960). Lemons' (1964) research was of an exploratory nature and showed that: (1) Brinell hardness was directly proportional to intercrystalline boundary area throughout the alpha brasses, (2) the linear relationship between hardness and boundary area could be used to distinguish the hardness of a grain per se from the hardness contribution of the grain boundary, (3) the average grain hardness per se was relatively insensitive to composition, (4) the grain boundary hardness contribution on the other hand, was strongly sensitive to composition, but not simply related to the amount of solute present in the alloys, and (5) further study would be required to understand completely these measurements.

In the year following the completion of this exploratory research, Rhines (1965) introduced and explained a model[1] whereby a grain boundary's resistance to plastic deformation could be directly related to grain boundary area. Although fundamental to the interpretation of a

---

[1]Appendix V is devoted to an abbreviated explanation of this model.

grain boundary's role in resistance to polycrystalline deformation, this model left several experimental facts unanswered. For instance: why is the grain boundary contribution to hardness sensitive to composition, and why isn't this sensitivity simply related to the amount of solute present in the alloy? In the research that is about to be presented, the writer has attempted to answer these questions by: (1) making the Brinell hardness versus boundary area measurements at several temperatures (77, 298, 573, and 873^{o}K); (2) carefully analyzing the crystal and crystal boundary contributions to hardness at all of these temperatures; (3) gleaning pertinent research findings from the metallurgical literature; (4) combining the experimental results, theory, and literature into a unified theory; and (5) repeating the basic experiments on another alloy system to test the generality of the information obtained from alpha brass.

1.40 Purpose and Scope of this Research

In spite of the fact that mechanical properties have been studied extensively as a function of various grain structure dimensions, no complete nor unambiguous

theory has evolved to explain the role of structure. Recently, advances in quantitative metallography have clearly defined the two- and three-dimensional measurements of grain dimensions with mathematical precision, thereby providing a sound basis for the understanding of problems in both the measurement and interpretation of structure relationships. Also, investigations have shown that indentation hardness is strongly sensitive to internal structure, and that this sensitivity implies an interaction between plastic-mechanical properties and structure per se. Therefore, the purpose of this research is to study the relationship between indentation hardness and intercrystalline boundary area as a function of composition and temperature in polycrystalline alpha brass. This is expected to lead to a better understanding of the role of structure in the deformation of metallic polycrystalline aggregates.

Alpha brass is ideally suited for this investigation because of: (1) the breadth of the alpha solid solubility range; (2) good working properties and the possibility of producing a wide range of grain size at all compositions;

(3) availability of high purity alloys; (4) the strong dependence of hardness upon grain size; (5) the vast amount of previous research upon its physical properties; and (6) the large amount of completed exploratory research into specific parameters that are of interest to the writer.

CHAPTER II

EXPERIMENTAL PROCEDURE

2.10 Materials and Specimen Production

In order to produce a wide range of uniform grain sizes in a series of alpha brass alloys (0-35 w/o zinc), materials were subjected to the following treatments. Base materials were received in the form of cast high purity 2x2x12 inch test bars.[1] The spectrographic analyses and nominal reference compositions of the seven test bars are given in Table I. Similar ingots of pure copper were made by melting and solidifying cathode sheet copper in a pure graphite crucible using a borax flux. All ingots were then cleaned and leveled by surface milling to: (1) eliminate inhomogenities, (2) produce parallel working surfaces for cold rolling, and (3) provide small chips at each composition for subsequent heat treating. Ingots were then reduced to sample size by the following procedure: (1) slice each ingot along its long axis and surface mill the

[1]Courtesy of Anaconda Brass Company.

TABLE I

Spectrographic Analysis of Alpha Brass Materials

MRL Number	w/o Copper	w/o Zinc
100	100.00	0.00
95	94.58	5.42
90	89.69	10.31
85	84.60	15.40
80	79.72	20.28
75	74.72	25.28
70	69.80	30.20
65	64.85	35.15

newly cut surfaces to produce 2x2x1.5 inch pieces; (2) strain each piece 33 per cent by cold rolling along the large faces; (3) separately heat treat each piece for one hour at 650°C; and (4) slice the 2.5x2.5x1 inch pieces into four equally sized specimens. Specimens of a given composition were heat treated together by incapsulating four at a time in a large iron chamber with similar composition chips. This procedure was followed for all heat treating to prevent dezincing and atmosphere contamination. Separate specimens were then cold rolled and heat treated varying amounts, producinga broad range of grain size at each composition. In general, grain sizes were fairly uniform, and any specimen that contained grains that varied greatly in size was discarded. This resulted in eight to twelve completely recrystallized specimens at each composition.

2.20 Metallographic Preparation and Measurements

2.21 Polishing and Etching

Polishing was done upon the rolled surface, giving a large flat surface for metallographic and hardness

measurements. The polishing procedure was: (1) remove sharp edges with a grinder; (2) level the large surfaces with a wet belt grinder to remove any irregularities; (3) grind with a slowly rotating wheel using No. 1 abrasive paper and kerosene lubricant; (4) hand grind using No.'s 0, 00, 000 and 0000 abrasive papers and kerosene lubricant; (5) polish one minute on a rotating polishing wheel using a nylon cloth, 6 micron diamond abrasive, and lapping oil lubricant; and (6) finish polish for two minutes using an AB microcloth, 1/4 micron diamond abrasive and lapping oil.

Etching easily revealed grain and twin boundaries using five parts ammonium hydroxide, five parts water, and two to five parts of 3 per cent hydrogen peroxide. Etching was generally done by swabbing the specimen surface with cotton soaked in etchant. This required from five to fifteen seconds exposure depending upon specimen grain size and composition. In general, etching time decreased with decreasing grain size, and increasing zinc content.

2.22 Boundary Area Determination

Grain and twin boundary area per unit volume (S_V) was determined by N_L measurements (where N_L is the average

number of grains and twin boundary intercepts with known length test line). The counting procedure was: (1) randomly place a polished and etched specimen on the stage of a Bausch and Lomb research type metallograph; (2) project the specimen image onto a screen that was marked with two bisecting fifteen centimeter test lines; (3) count test line intersections with grain and twin boundaries, counting tangent intersections as one rather than two intersections; (4) lift the specimen, randomly rotate and translate it to a new position on the metallograph stage; and (5) repeat this procedure fifteen times on each specimen. Magnification was determined using the standard formula for projection along the metallograph camera extension (or where the screen was placed). A minimum number of required counts was obtained by increasing the number from one to eighty and observing the fluctuations in boundary area (S_v). After fifteen counts the result was within 5 per cent of the value obtained after eighty counts. Boundary areas were calculated through the quantitative metallography relation $S_v = 2N_L$. Specifically: $S_v = 2N_L$ = two times the product of the magnification and the average

number of boundary intercepts per fifteen centimeter test line, divided by the length of the test line.

The intercrystalline boundary area measurement includes both grain and twin boundaries counted at equal value. If subboundaries were present in any of the alloys they also would be included in this measurement, but none were found. The writer did find that second order annealing twins could be distinguished within first order twins by illuminating with polarized light. These second order twins were found only in alloy compositions from copper to 80-20 copper-zinc. Therefore, these alloys were measured for N_L using both bright field and polarized light illumination. The second order twins did add to the value of N_L and were therefore included in the boundary area measurements.

To ascertain the regularity of grain size throughout the specimens, a check was made of boundary area measurements on transverse sections. No appreciable change was found on the cross section as long as the specimens were completely recrystallized.

2.30 Brinell Hardness Measurements

2.31 Hardness at Room Temperature

Hardness impressions were made at room temperature with a Model UK 300-T Brinell hardness tester using a 500

kilogram load, 10 millimeters in diameter hardened steel ball, and a 30 second test time (500/10/30). Four impressions were located at equal distances from the specimen corners along the diagonals of the large polished surface. The diameter of each impression was measured using a calibrated Bausch and Lomb 20x microscope. With this microscope it was possible to measure 0.02 millimeters accurately. Three diameters, separated at 60 degree intervals were averaged for each impression and the four impressions were finally averaged for each specimen. Brinell Hardness Numbers were obtained from standard tables. A standard brass test block was checked before and after all hardness testing, showing no machine error.

Some interest was generated in the hardness along surfaces other than the rolling plane. Therefore a check was made along several cuts placed at 90 degrees to the rolling plane. Transverse and rolling plane hardness measurements were in agreement.

2.32 Hardness at 77, 298, 573, and 873°K

Four specimens spanning the grain size range available at each composition were chosen for testing at temperatures other than room temperature. Brinell Hardness Number was obtained from a single hardness impression at each test temperature. At 77°K, both the specimen and indenter were immersed in liquid nitrogen, using the regular test conditions (500/10/30). Testing at higher temperatures required a specially rigged chamber. This chamber contained the specimen, powdered graphite, and metal chips of the same composition as the specimen. The purpose of the graphite and chips was to provide a protective atmosphere during the high temperature testing. The specimen was rigidly located in the test chamber by four set screws, and rested on the bottom of the chamber. This accurately located the specimen with respect to the indenter axis and held it in place during the test. The complete chamber, including the indenter was heated to test temperature, placed in the Brinell machine for testing, then naturally cooled to room temperature. Extensive pretest investigations were run to determine the correct heat up and test time. Twenty

minutes was found to be an acceptable heat up time at both of the elevated temperatures. At 573°K, hardness test conditions were (500/10/30), while at 873°K the test time was reduced to three seconds (500/10/3). The reduced time at 873°K was to prevent the indenter from sinking below one-half of the ball diameter. After all of the high temperature testing was complete, a final hardness test was made at room temperature to ascertain how much the specimen had changed during these tests. The final room temperature hardness was almost the same as the hardness before the high temperature tests. The reason for this was:(1) that the original grain structure was completely recrystallized and therefore had changed very little during the tests, and (2) that very little specimen contamination had taken place. Specimen histories, boundary areas, and hardnesses are summarized in Tables II through IX.

2.40 Meyer Hardness Measurements

2.41 Hardness at 500 Kilograms Load

Meyer Hardness Number is expressed as the load per projected indentation surface area rather than the load per curved surface area used in the Brinell Hardness Number

TABLE II

Pretreatment, Boundary Area and Hardness Data Summary for Pure Copper

Specimen	Per Cent CW*	Heat Treatment	S_V+	BHN≠			
				77°K	298°K	573°K	873°K 298°K$_f$
100-1	10	1.5 hr. @ 700°C	347.0		37.7		
	20	1.0 hr. @ 700°C					
		0.5 hr. @ 800°C					
100-2	20	1.5 hr. @ 700°C	458.6	47.2	39.4	34.9	21.6
	10	1.0 hr. @ 700°C					
	30	2.0 hr. @ 600°C					
100-3	30	1.5 hr. @ 700°C	301.2		37.3		
	5	1.0 hr. @ 700°C					
		0.5 hr. @ 800°C					
100-4	40	1.5 hr. @ 700°C	895.4	53.1	40.0	34.9	23.6
	23	1.5 hr. @ 500°C					
100-5	10	1.5 hr. @ 850°C	286.4		37.0		
	10	1.0 hr. @ 700°C					
100-6	20	1.5 hr. @ 850°C	270.9	44.1	37.3	32.1	20.0
100-7	30	1.5 hr. @ 850°C	209.2		38.1		
	20	2.0 hr. @ 600°C					
100-8	40	1.5 hr. @ 841°C	45.6	43.9	35.5	32.3	20.3

* Per Cent CW - Per cent cold work by rolling.
+ S_V - Surface area per unit volume = grain + twin boundary area (cm^2/cm^3).
≠ BHN - Brinell Hardness Number (Kg/mm^2).

TABLE III

Pretreatment, Boundary Area and Hardness Data Summary for 95-5 Copper-Zinc

Specimen	Per Cent CW	Heat Treatment	S_V+	BHN				
				77°K	298°K	573°K	873°K	298°K_f
95-3	25	3 hr. @ 500°C	759.3		45.2			
95-4	50	3 hr. @ 500°C	1208.5	59.4	48.9	42.0	31.2	48.0
95-6	15	1 hr. @ 600°C	507.1	54.8	44.2	39.1	28.7	43.4
95-7	35	1 hr. @ 600°C	766.2		45.0			
95.8	50	1 hr. @ 600°C	893.1	57.5	46.6	40.2	30.9	46.9
95-10	10	1 hr. @ 700°C	284.2		41.6			
95-11	25	1 hr. @ 700°C	494.5		43.3			
95-12	50	1 hr. @ 700°C	565,6		44,9			
95-13	10	1 hr. @ 800°C	280.1		41.7			
95-14	25	1 hr. @ 800°C	361.5		42.3			
95-15	35	1 hr. @ 800°C	352.3	52.8	42.2	37.7	28.3	42.4
95-16	50	1 hr. @ 800°C	367.7		42.4			

TABLE IV

Pretreatment, Boundary Area and Hardness Data Summary for 90-10 Copper-Zinc

Specimen	Per Cent CW	Heat Treatment	S_V+	BHN				
				77°K	298°K	573°K	873°K	$298°K_f$
90-3	25	3 hr. @ 500°C	892.8		52.0			
90-4	50	3 hr. @ 500°C	1618.5	67.7	55.9	48.0	31.5	53.4
90-6	15	1 hr. @ 600°C	581.0	59.0	48.0	44.4	30.9	47.5
90-7	35	1 hr. @ 600°C	839.5	60.9	50.9	44.9	30.7	50.3
90-8	50	1 hr. @ 600°C	964.2		53.1			
90-10	10	1 hr. @ 700°C	366.6		46.1			
90-11	25	1 hr. @ 700°C	626.4		48.3			
90-12	50	1 hr. @ 700°C	635.3		49.3			
90-13	10	1 hr. @ 800°C	353.8		45.4			
90-14	25	1 hr. @ 800°C	218.5		44.9			
90-15	35	1 hr. @ 800°C	283.1	55.4	45.1	40.0	30.0	44.0
90-16	50	1 hr. @ 800°C	260.3		44.9			

TABLE V

Pretreatment, Boundary Area, and Hardness Data Summary for 85-15 Copper-Zinc

Specimen	Per Cent CW	Heat Treatment	S_v+	BHN				
				77°K	298°K	583°K	873°K	298°K$_f$
85-3	25	3 hr. @ 500°C	1562.5		59.6			
85-6	15	1 hr. @ 600°C	821.1		50.9			
85-7	35	1 hr. @ 600°C	1402.2		57.0			
85-8	50	1 hr. @ 600°C	1383.9	70.0	57.2	51.2	31.7	56.8
85-10	10	1 hr. @ 700°C	646.3		48.0			
85-11	25	1 hr. @ 700°C	763.8	64.6	53.1	48.0	32.1	51.5
85-12	50	1 hr. @ 700°C	522.3	61.3	51.3	46.9	32.3	51.8
85-13	10	1 hr. @ 800°C	310.9		45.4			
85-14	25	1 hr. @ 800°C	219.0	56.8	45.4	40.2	31.4	44.4
85-15	35	1 hr. @ 800°C	178.6		45.2			
85-16	50	1 hr. @ 800°C	205.9		45.1			

TABLE VI

Pretreatment, Boundary Area, and Hardness Data Summary for 80-20 Copper-Zinc

Specimen	Per Cent CW	Heat Treatment	S_V+	BHN				
				77°K	298°K	583°K	873°K	298°K$_f$
80-2	15	1 hr. @ 600°C	1114.9		54.8			
80-3	35	1 hr. @ 600°C	1459.5	73.0	59.8	42.5	32.4	58.6
80-4	50	1 hr. @ 600°C	1046.0	68.2	57.3	51.8	32.8	60.1
80-7	25	3 hr. @ 500°C	1755.5		61.7			
80-10	10	1 hr. @ 700°C	489.5		48.2			
80-11	25	1 hr. @ 700°C	537.1		50.6			
80-12	50	1 hr. @ 700°C	403.6	60.9	48.6	44.1	31.4	48.3
80-13	10	1 hr. @ 800°C	158.4		42.7			
80-14	25	1 hr. @ 800°C	236.3	56.8	43.8	40.2	29.8	43.0
80-15	35	1 hr. @ 800°C	134.7		43.3			
80-16	50	1 hr. @ 800°C	161.3		44.6			

TABLE VII

Pretreatment, Boundary Area, and Hardness Data Summary for 75-25 Copper-Zinc

Specimen	Per Cent CW	Heat Treatment	S_v+	BHN				
				77°K	298°K	583°K	873°K	298°K$_f$
75-3	25	3 hr. @ 500°C	1033.1		61.5			
75-4	50	3 hr. @ 500°C	1454.0		67.3			
75-7	35	1 hr. @ 600°C	1047.0	76.2	60.1	53.8	25.9	59.0
75-8	50	1 hr. @ 600°C	765.8	73.6	58.6	53.8	28.4	57.5
75-10	10	1 hr. @ 700°C	491.0		47.2			
75-11	25	1 hr. @ 700°C	374.8		48.6			
75-12	50	1 hr. @ 700°C	330.7	63.8	46.7	44.9	33.2	50.6
75-13	10	1 hr. @ 800°C	157.2		42.0			
75-14	25	1 hr. @ 800°C	172.6	56.8	41.7	37.5	28.4	41.5
75-15	35	1 hr. @ 800°C	151.7		40.9			
75-16	50	1 hr. @ 800°C	131.7		41.1			

TABLE VIII

Pretreatment, Boundary Area, and Hardness Data Summary for 70-30 Copper-Zinc

Specimen	Per Cent CW	Heat Treatment	S_V+	BHN				
				77°K	298°K	573°K	873°K	298°K$_f$
70-3	25	3 hr. @ 500°C	828.8		56.1			
70-4	50	3 hr. @ 500°C	1575.4	83.2	67.0	58.6	25.4	62.9
70-6	15	1 hr. @ 600°C	731.8		51.7			
70-7	35	1 hr. @ 600°C	826.2		55.1			
70-8	50	1 hr. @ 600°C	771.6	69.1	54.1	51.8	29.9	50.9
70-10	10	1 hr. @ 700°C	433.9		46.1			
70-11	25	1 hr. @ 700°C	365.9	64.6	48.1	42.9	24.1	51.2
70-12	50	1 hr. @ 700°C	293.2		45.9			
70-13	10	1 hr. @ 800°C	115.5		40.2			
70-14	25	1 hr. @ 800°C	126.8		40.9			
70-15	35	1 hr. @ 800°C	130.1	56.8	40.9	38.3	26.9	39.2
70-16	50	1 hr. @ 800°C	153.0		41.5			

TABLE IX

Pretreatment, Boundary Area, and Hardness Data Summary for 65-35 Copper-Zinc

Specimen	Per Cent CW	Heat Treatment	S_v+	BHN				
				77°K	298°K	573°K	873°K	298°K$_f$
65-4	50	3 hr. @ 500°C	1733.4	79.6	64.4	56.8	23.6	61.7
65-5	15	1 hr. @ 600°C	731.7		52.8			
65-7	35	1 hr. @ 600°C	717.8	73.6	54.6	52.8	20.9	56.5
65-8	50	1 hr. @ 600°C	739.9		54.4			
65-10	10	1 hr. @ 700°C	364.8		47.7			
65-11	25	1 hr. @ 700°C	155.9		43.8			
65-12	50	1 hr. @ 700°C	228.8	62.5	47.6	43.6	21.2	46.9
65-13	10	1 hr. @ 800°C	316.4		50.0			
65-14	25	1 hr. @ 800°C	463.0	65.9	51.2	46.4	20.5	50.3
65-15	35	1 hr. @ 800°C	501.8		53.1			
65-16	50	1 hr. @ 800°C	376.6		51.3			

Thus, all of the Brinell hardness data at 500 kilograms load could be converted easily to Meyer hardnesses by a simple calculation. This was done, and, as was mentioned earlier, the results were within 1 per cent. Therefore, a general presentation of these data at all alpha brass alloy compositions is not included.

2.42 Hardness at 1000 Kilograms Load

The Meyer analysis of the load versus impression diameter relationship requires hardness tests at at least two different loads. Therefore the writer decided to measure Meyer hardness using a 1000 kilogram load, 10 millimeters in diameter ball, and 30 second test time (1000/10/30). The only materials available for this investigation were the previously described Brinell hardness specimens. Since four of the eight to twelve available specimens were already in use for the elevated temperature investigation, the range of boundary area was narrow and not always the same. This later proved to be a limiting condition in the use of this analysis. Also, to cut down on the number of tests, and to best utilize the available specimens, compositions of 5, 15, 25, and 35 w/o zinc were selected for this survey.

Hardness impressions were made with the Model UK300-T Brinell hardness tester. The impressions were placed along the large surface of the specimens, using a single impression to determine each hardness number. It was impossible to make more than one indentation at 1000 kilograms because of the limited specimen surface area. Care was taken to make sure that the specimens were thick enough to prevent any anvil effect. Impression diameters were measured by the same method as was previously explained for the Brinell tests. No standard tables were available for the Meyer Hardness Numbers, so all numbers were calculated using the Meyer formula $MHN = 4L/\pi d^2$, where L = load in kilograms, and d = chordal diameter of the hardness impression in millimeters.

2.43 Meyer Pretest Hardness and Strain Hardening Coefficient

The Meyer formula $L = kd^n$ is easily analyzed for k and n by expanding in terms of logarithms, that is, $\log L = \log k + n \log d$. Log L is then plotted versus log d which gives the value of log k and n as the intercept and slope respectively. The load k is converted to

pretest hardness $(MHN)_k$ by dividing k by the constant projected area when d equals one millimeter. Therefore, pretest hardness $(MHN)_k$ is always proportional to the load k because the impression area is constant. The strain hardening coefficient (n) is taken directly from the log L versus log d relationship without any conversions.

2.44 Strain Sensitivity Limit of Boundary Area

Another measurement taken from the log L versus log d graphs is the value of load and diameter where the various boundary area relationships merge to a single line. This value is interpreted as a measure of the amount of deformation required to cause the mechanical effects of grain size to be unrecognizable in a hardness test. This material state is often called the fully hard condition. This value of load and diameter is converted to a Meyer Hardness Number $(MHN)_L$ so that comparisons can be made between alloy compositions.

Meyer Hardness Number at 500 and 1000 kilogram loads $(MHN)_{500}$ and $(MHN)_{1000}$, pretest hardness number $(MHN)_k$, strain hardening coefficient (n), and the strain sensitivity limit of boundary area $(MHN)_L$ are summarized in Table X.

TABLE X

Meyer Hardnesses and Strain Hardening Coefficients for Recrystallized Alpha Brass

Specimen	S_v (cm^2/cm^3)	MHN_{500} (kg/mm^2)	MHN_{1000} (kg/mm^2)	MHN_K (kg/mm^2)	n (kg/mm^2)	MHN_L (kg/mm^2)
95-2	226.9	39.8	48.0	14.2	2.734	
95-14	361.5	44.1	51.0	21.9	2.525	
95-11	494.5	45.0	53.1	19.9	2.617	68
95-3	759.3	47.0	53.5	26.0	2.455	
95-7	766.2	46.8	53.7	24.4	2.498	
95-4	1205.0	50.5	57.7	37.3	2.282	
85-2	183.9	43.2	51.4	17.6	2.666	
85-13	310.9	47.0	55.3	21.3	2.608	
85-10	646.3	49.7	57.4	25.4	2.527	110
85-6	821.1	52.6	60.5	28.0	2.504	
85-3	1562.5	61.4	66.4	45.7	2.253	
75-2	278.7	40.6	47.1	19.2	2.544	
75-11	274.8	50.3	58.2	25.5	2.534	
75-10	491.0	48.9	55.3	28.0	2.433	130
75-3	1033.1	63.4	69.5	44.3	2.310	
75-4	1454.0	68.9	75.8	48.4	2.317	
65-2	265-8	42.7	50.4	18.6	2.617	
65-10	364.8	49.4	57.2	25.0	2.534	75
65-15	501.8	60.7	35.7	35.7	2.350	
65-6	731.7	54.4	59.7	37.4	2.305	

2.50 Vickers Microhardness

Microhardness measurements were made on several series of alpha brass specimens. All testing was done at room temperature using a Vickers 136 degree diamond pyramid indenter, 50 gram test load, 30 second test time, and always indenting on a polished and etched surface. The microhardness tester was a Kentron. A certified brass microhardness test block was checked before and after all testing and showed no machine error.

2.51 Grain Center Measurements on Annealed Alloys

The first series of microhardness tests consisted of measurements on large grain size specimens of completely recrystallized alpha brass. These measurements were made by selectively placing microhardness impressions in the center of twenty-five grains at each composition. Care was taken to choose grains of approximately the same size for all tests. The reason for testing so many grain centers at each composition was so that the average microhardness number would eliminate the crystal anisotropy.

2.52 Grain Center and Grain Boundary Comparisons on Annealed Alloys

Another series of microhardness measurements was made to compare grain centers and grain boundaries for the 5, 15, 25, and 35 w/o zinc alloys of alpha brass. Microhardness impressions were made along twenty-five grain and twin boundaries, and also at the center of twenty-five grains. These specimens were not the same ones used in the previous microhardness survey, but were similar in that they were also completely recrystallized and of a large grain size. The microhardness impressions at the grain and twin boundaries were located directly over the boundary traces on the polished and lightly etched specimen surface.

2.53 Grain Center and Grain Boundary Comparisons on Strained Alloys

To extend the microhardness survey beyond the analysis of completely recrystallized alloys, the writer decided to make microhardness measurements on a series of strained alloys in hope that a comparison of grain centers and grain boundaries might correlate with results from Brinell hardness measurements. The alloys studied were the previously investigated compositions of 5, 15,

25, and 35 w/o zinc. To strain the test material, a Brinell impression (500/10/30) was placed in the center of the large square polished surface at each composition. Microhardness impressions were then placed at grain centers and grain and twin boundaries along the diagonals of the specimen surface, locating each impression with respect to the edge of the Brinell impression. The purpose of this particular test procedure was two-fold: (1) to check the relative microhardness of grain centers and boundaries on strained alloys, and (2) to check the distance that the disturbed or strained condition extended along the recrystallized specimens' surface.

Microhardness measurements are summarized for all of the above mentioned tests in Table XI.

TABLE XI

Vickers Microhardness Measurements on Recrystallized and Strained Alloys of Alpha Brass

Specimen	S_V (cm^2/cm^3)	VHN(kg/mm^2)			
		Recrystallized		Strained	
		Av.of 25 grain centers	Av.of 25 grain boundaries	Av.of 25 grain centers	Av.of 25 grain boundaries
100-5	286.4	51.9			
95-10	284.2	53.5			
95-A	227.0	55.4	56.6	56.2	57.2
90-14	218.5	69.9			
85-13	310.9	77.4			
85-B	184.0	64.2	66.9	66.7	65.7
80-13	158.4	65.1			
75-11	374.8	82.0			
75-C	278.0	65.2	65.5	69.1	67.6
70-14	126.8	78.7			
65-13	316.4	79.4			
65-D	266.0	67.5	67.7	69.8	69.7

CHAPTER III

EXPERIMENTAL RESULTS

3.10 Brinell Hardness Versus Boundary Area Relationships

Brinell Hardness Number is linearly related to boundary area over a temperature range of at least 77 - 873°K, throughout the alpha solubility limits of the copper-zinc system, Figures 1 through 8.

The linear relationship between hardness and boundary area can be expressed by the equation $y = mx + b$ where y = BHN, x = boundary area, m = slope, and b = intercept at zero boundary area. The intercept at zero boundary area (b) is the hardness without grain or twin boundaries and is interpreted as being equivalent to that of a single crystal hardness that is averaged over all crystal orientations. The hardness contribution of boundary area is obtained by subtracting the average single crystal hardness from polycrystalline hardness. Thus, a measure of the boundary area hardness contribution is the slope (m) of the hardness versus boundary area relationship. These separations are shown schematically in Figure 9. It must be emphasized

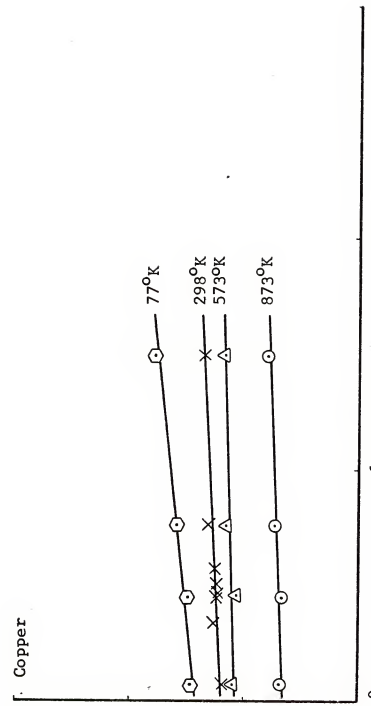

Figure 1. Brinell Hardness Number versus grain plus twin boundary area for pure copper at 77, 298, 573 and 873°K

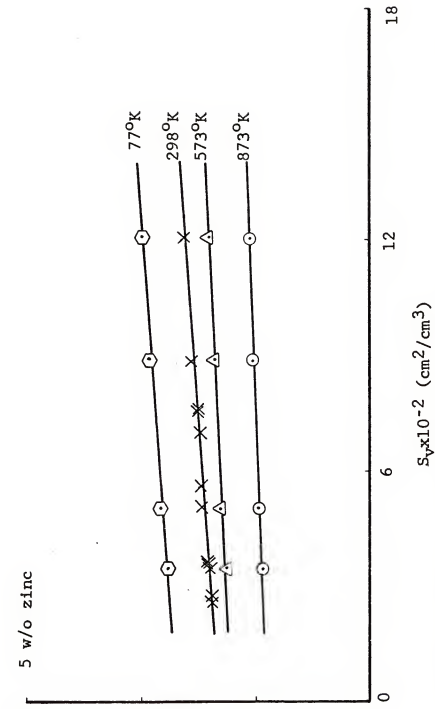

Figure 2. Brinell Hardness Number versus grain plus twin boundary area for 5 w/o zinc alpha brass at 77, 298, 573 and 873°K

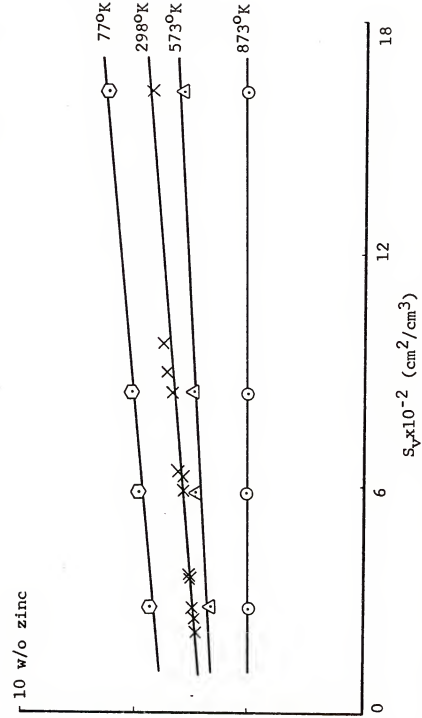

Figure 3. Brinell Hardness Number versus grain plus twin boundary area for 10 w/o zinc alpha brass at 77, 298, 573 and 873°K

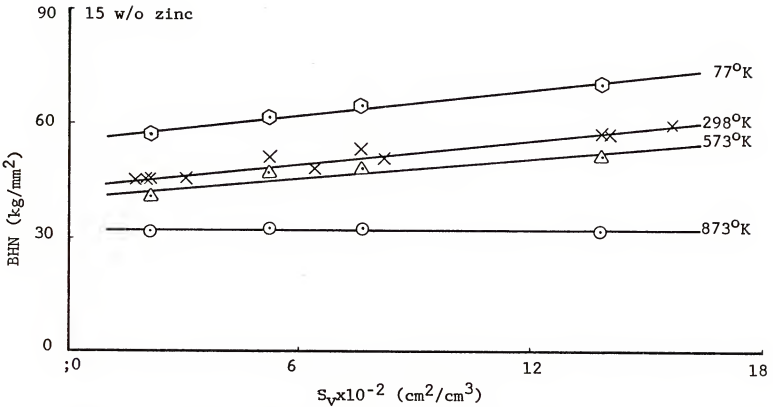

Figure 4. Brinell Hardness Number versus grain plus twin boundary area for 15 w/o zinc alpha brass at 77, 298, 573 and 873°K

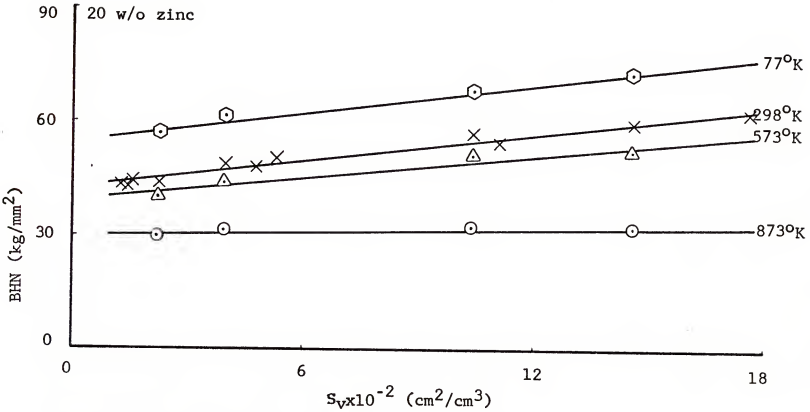

Figure 5. Brinell Hardness Number versus grain plus twin boundary area for 20 w/o zinc alpha brass at 77, 298, 573 and 873°K

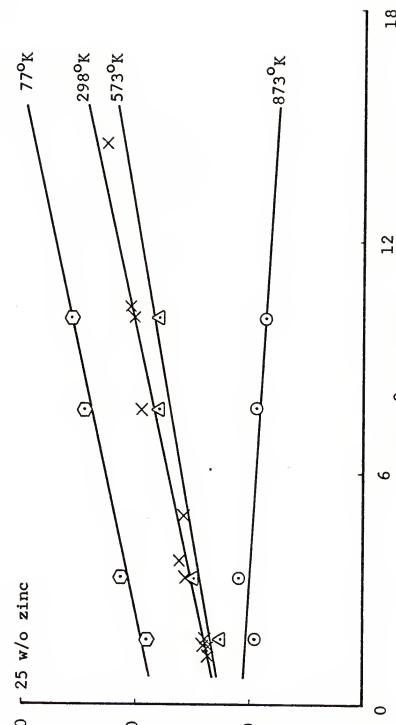

Figure 6. Brinell Hardness Number versus grain plus twin boundary area for 25 w/o zinc alpha brass at 77, 298, 573 and 873°K

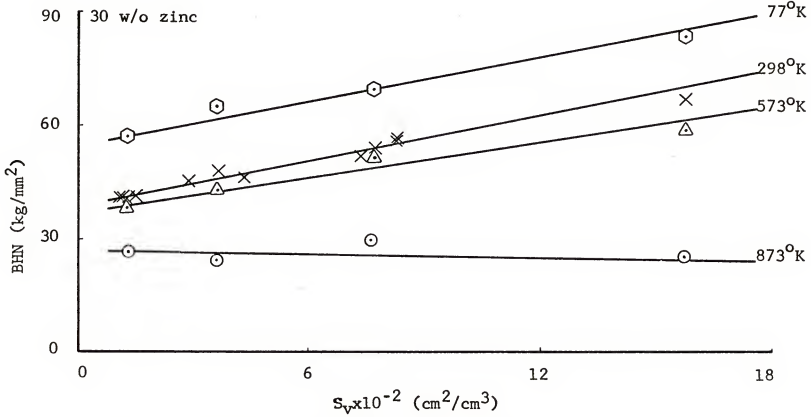

Figure 7. Brinell Hardness Number versus grain plus twin boundary area for 30 w/o zinc alpha brass at 77, 298, 573 and 873°K

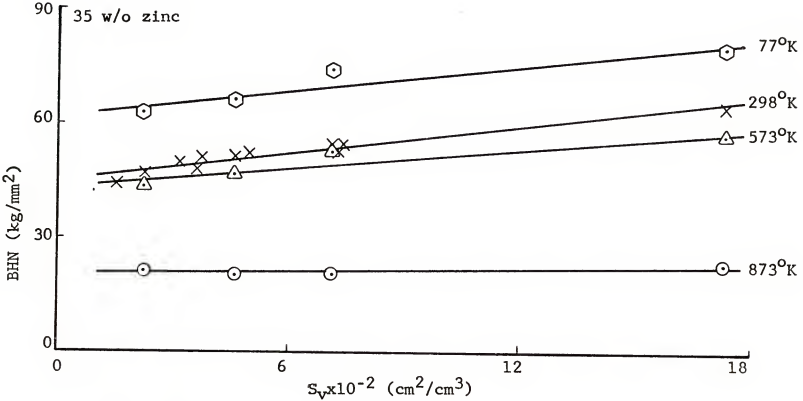

Figure 8. Brinell hardness Number versus grain plus twin boundary area for 35 w/o zinc alpha brass at 77, 298, 573 and 873°K

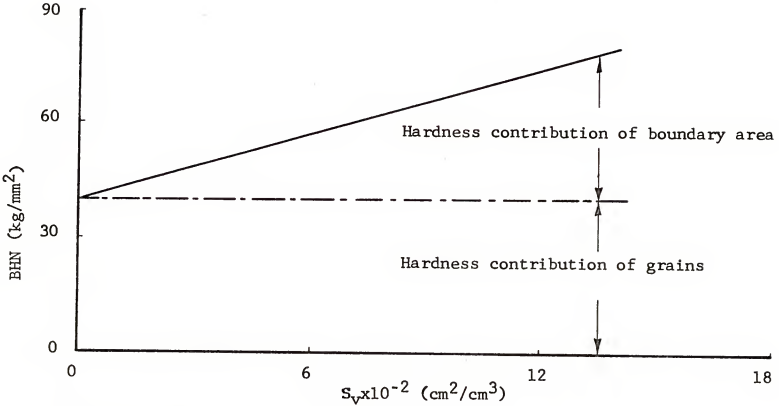

Figure 9. Schematic representation of the separation of average grain and boundary area contributions to hardness for a Brinell Hardness Number versus grain plus twin boundary area graph

here that hardnesses measured at the same high value of boundary area (polycrystalline hardness) and the slopes of the hardness versus boundary area relationships would show the same relative behavior as a function of composition, although there is a difference in what they measure. The slope measures the hardness contribution of the boundary area per se, while the polycrystalline hardness is the sum of the average crystal and crystal boundary hardness contributions.

3.11 Brinell Hardness at Zero Boundary Area

Average crystal hardness is relatively insensitive to zinc concentration, with each alloy showing a regular hardness decrease with increasing temperature, Figure 10. The shape of each average crystal hardness-composition relationship is also important and will be considered in detail in the discussion.

3.12 Contribution of Boundary Area to Brinell Hardness

Boundary area contribution to hardness at 77 and 298^{o}K increases slowly up to about 15 w/o zinc, then rises

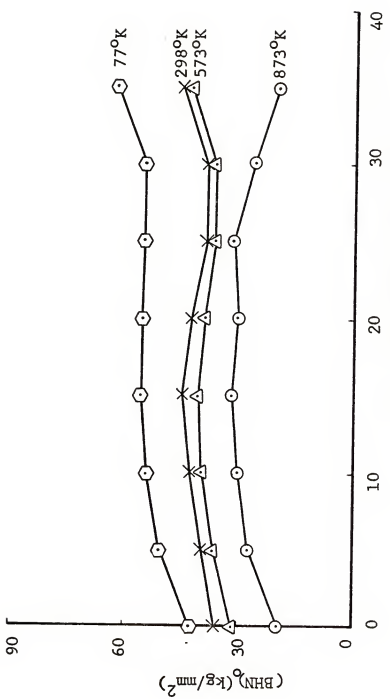

Figure 10. Average crystal hardness versus zinc concentration in alpha brass at 77, 298, 573 and 873°K

to a maximum at 25-30 w/o zinc. At 573°K, the maximum hardness contribution at 25-30 w/o zinc decreases, completely disappearing at 873°K, Figure 11.

3.20 Meyer Hardness

In the Meyer analysis of 1908, both the pretest hardness $(MHN)_k$ and the strain hardening coefficient (n) were considered to be constants that depended only upon (1) the type of material, and (2) the physical condition of the material. The writer found that both of these parameters were sensitive to boundary area in alpha brass. To show this, a typical set of experimental data from a 15 w/o zinc alpha brass alloy and Meyer's formula relating load and diameter are presented in Figure 12. Referring to Figure 12, note that a linear relationship is determined at each boundary area, and that the slope decreases with increasing boundary area.

3.21 Meyer Hardness Versus Boundary Area of 1000 Kilogram Load

The Meyer Hardness Numbers measured at 1000 kilograms loads were directly proportional to boundary area at all compositions of alpha brass tested in the Meyer

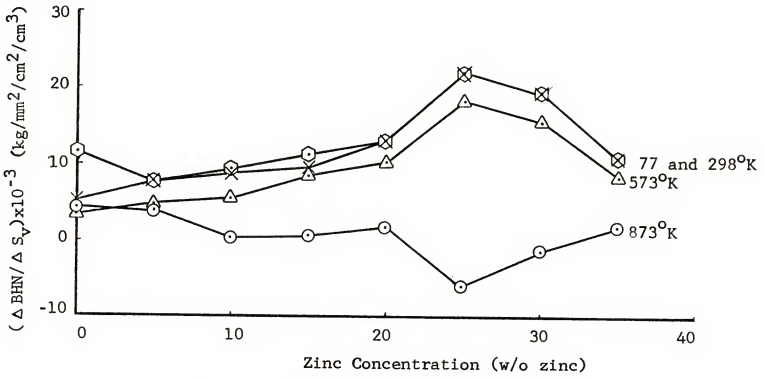

Figure 11. Contribution of boundary area to Brinell Hardness versus zinc concentration in alpha brass at 77, 298, 573 and 873°K

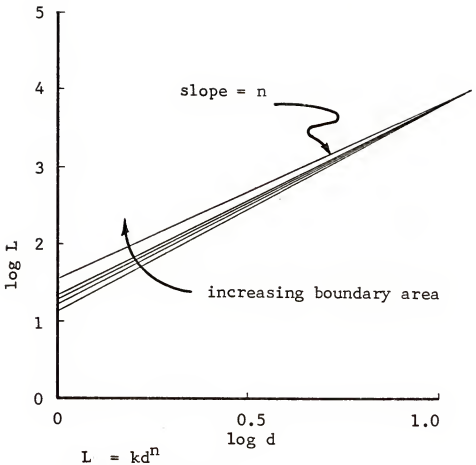

$L = kd^n$
L = load in kg
d = diameter of impression (mm)
k = load in kg when d = 1mm
n = strain hardening coefficient

Figure 12. Meyer equation relating load and impression diameter, and a log load versus log diameter graph for several different boundary area specimens of 15 w/o zinc alpha brass

analysis. Although the hardness numbers were higher, a comparison of crystal and crystal boundary hardness contributions as a function of alloy composition, shows the same results as obtained at the 500 kilogram loads. These data are summarized in Table X.

3.22 Meyer Pretest Hardness

Figure 13 shows the change in Meyer pretest hardness $(MHN)_k$ with boundary area for the 5, 15, 25, and 35 w/o zinc alloys of alpha brass. The change in $(MHN)_k$ with boundary area appears to be highest for 35 w/o zinc, showing a steady and regular decrease with decreasing zinc content. The range of boundary area sampled in these tests becomes very important in these results in that it limits comprehensive comparisons between alloys.

3.23 Meyer Strain Hardening Coefficient

The Meyer coefficient of strain hardening (n) is plotted as a function of boundary area in Figure 14 for the 5, 15, 25, and 35 w/o zinc alloys of alpha brass. Comparing compositions, note that for the 25 w/o zinc alloys of alpha brass, n is larger at high values of

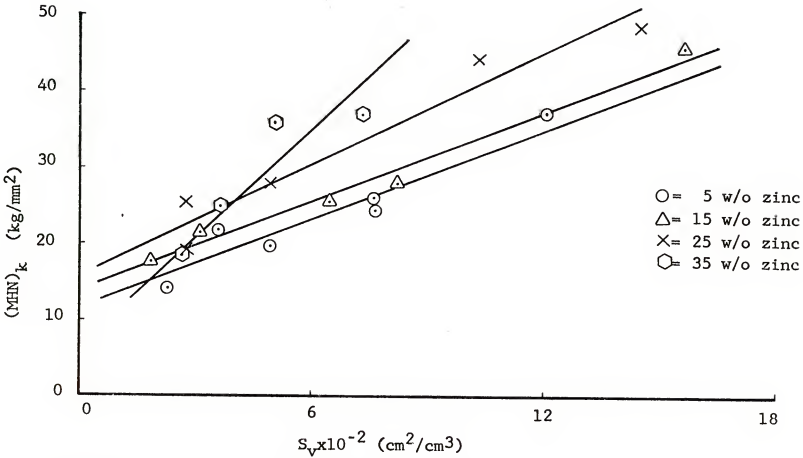

Figure 13. Meyer pretest hardness versus grain plus twin boundary area for the 5, 15, 25, and 35 w/o zinc compositions of alpha brass

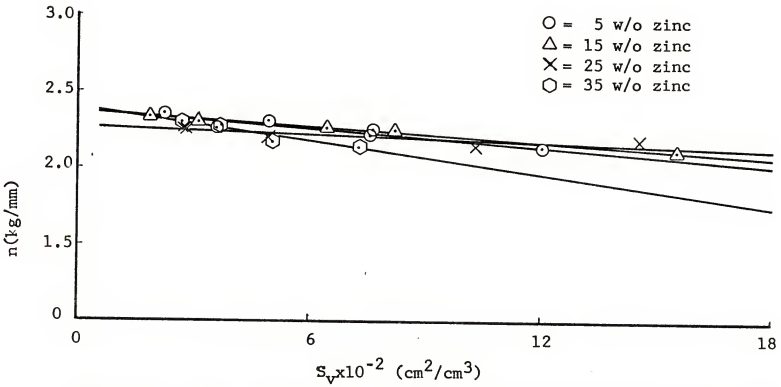

Figure 14. Meyer coefficient of strain hardening versus grain plus twin boundary area for the 5, 15, 25 and 35 w/o zinc alloys of alpha brass

boundary area and smaller at low values of boundary area. Also, the slope of the n versus boundary area relationship is smallest for the 25 w/o zinc compositions.

3.24 Meyer Strain Sensitivity Limit of Boundary Area

Meyer log L versus log d diagrams are plotted for the 5, 15, 25, and 35 w/o zinc alloy compositions and all boundary areas are tested in the current Meyer analysis in Figure 15, part (a) through part (d). The important point to be made with these diagrams is that the value of load and diameter where all of the boundary area lines merge is highest for the 25 w/o zinc alloy. Specific numbers for $(MHN)_L$ were included in Table X.

3.30 Vickers Microhardness

3.31 Grain Center Microhardness Measurements on Annealed Alloys

Figure 16 shows a plot of average microhardness number as a function of zinc content in recrystallized alpha brass. The average microhardness measurements for grain centers are relatively insensitive to alloy composition, showing a slight increase with increasing zinc content.

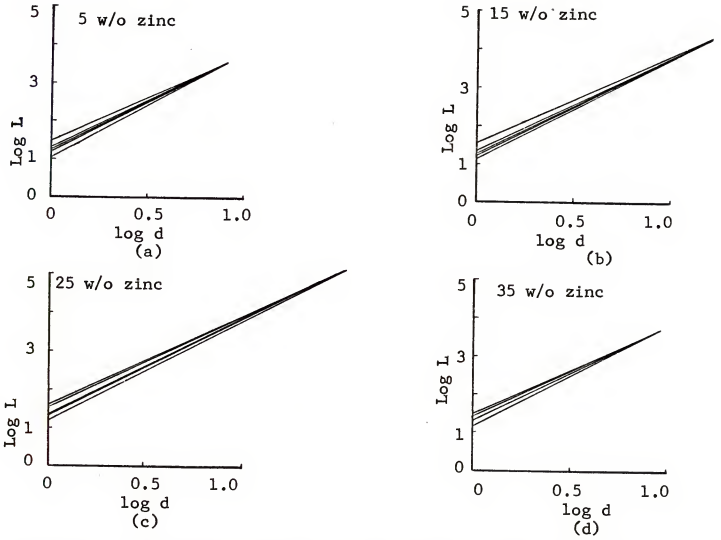

Figure 15. Meyer log load versus log diameter graphs for all of the different specimens of 5, 15, 25 and 35 w/o zinc alpha brass

Figure 16. Average crystal microhardness versus zinc concentration for alpha brass.

3.32 Grain Center and Grain Boundary Microhardness Comparisons on Annealed Alloys

Average microhardness numbers of both grain centers and boundaries are compared for the 5, 15, 25, and 35 w/o zinc alpha brass alloys in Figure 17. The average microhardness number increase of the boundary (shown by the x's) over the grain center is small, approximately 4 per cent, and constant at all compositions. The grain center measurements collected in this survey were found to be in good agreement with the previous grain center measurements when similar compositions are compared.

3.33 Grain Center and Boundary Microhardness Comparisons on Strained Alloys

Microhardness numbers for the 5, 15, 25, and 35 w/o zinc alpha brass alloys are plotted versus distance from the Brinell impression perimeter for both grain centers and boundaries in Figure 18. The x's represent the boundary and the dots represent the grain centers measurements. Several trends can be read from this data, but in general, the broad scatter band precludes any complete analysis. The results worth mentioning are: (1) the average microhardness number is approximately the

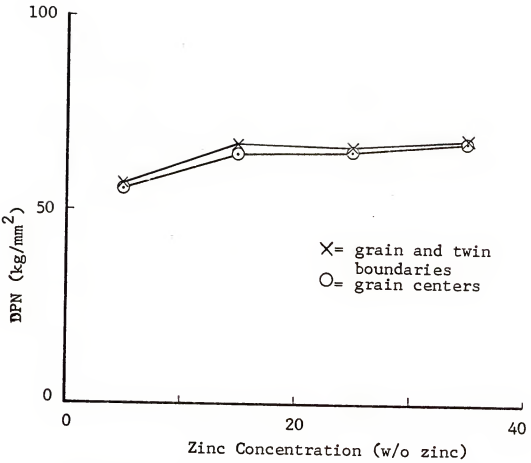

Figure 17. Average microhardness number versus zinc concentration for grain centers and boundaries annealed in alpha brass

× = grain and twin boundaries
· = grain center
----- = average of boundary measurements
——— = average of grain center measurements

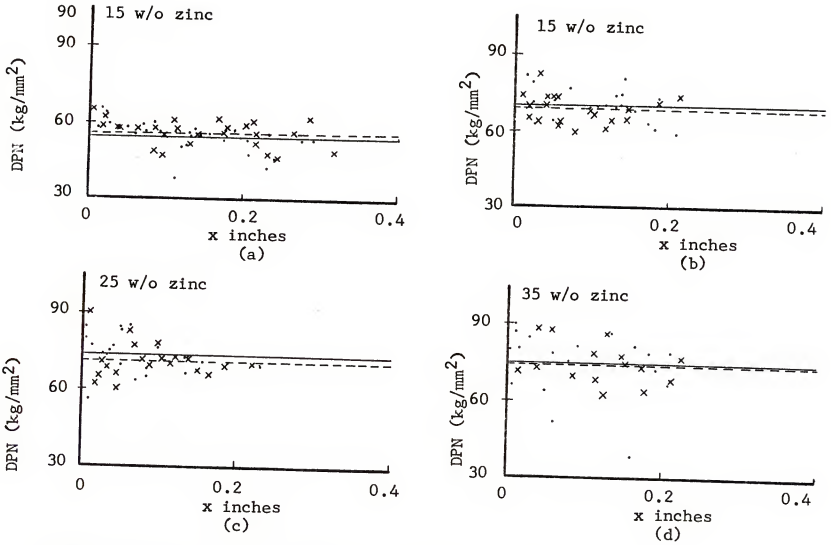

Figure 18. Microhardness number versus distance from a Brinell impression perimeter for the 5, 15, 25 and 35 w/o zinc alloys at alloy alpha brass

same at each composition when annealed and strained conditions are compared, (2) both the grain center and grain boundary microhardness show an increase with the amount of strain present, and (3) the microhardness does increase near the edge of the Brinell impression but the magnitude of the increase and the distance of strain influence along the specimen surface could not be meaningfully measured because of experimental scatter in the data.

CHAPTER IV

DISCUSSION

The primary objective of this research has been to discover what it is about fine grained materials that makes them harder and stronger than coarse grained materials. It has been deduced through information in the literature, as will be demonstrated presently, that only the plastic and not the elastic responses of metals to a deforming force is sensitive to grain size. Some investigators have chosen to correlate what they imagine to be a measure of the grain diameter with mechanical properties, while others have used the grain surface area in this correlation. Either approach leads to a qualitatively similar result. An analysis of the geometry of the measurements, however, shows that the most frequently used schemes for measuring either "grain diameter" or grain boundary area, were in fact, measurements for some property of the grain boundary as a surface. Recent developments in quantitative metallography have made

it possible to measure grain boundary area with great precision. Since this parameter can be defined exactly, and since it does show lineal correlation with hardness, the objective of this research has been focused upon the explanation of the resistance to indentation (as in a hardness test) as a function of intercrystalline boundary area.

A survey of the alpha alloys of the system copper-zinc has brought forth the observation that the hardness of fine grained alloys maximizes sharply near 25 w/o zinc. The same is not true of the copper-zinc series when grain boundaries are absent, so that it is apparent that there is something about the interaction of the hardness indent with grain boundaries of 25 w/o zinc that is different from the reaction at other compositions. This is particularly interesting because it offers an opportunity to gain insight into the fundamental reason for grain boundary hardening by finding what structural feature of the 25 w/o zinc alloy may be unique with respect to the copper-zinc series. Of all the properties of a crystal that have been investigated in this composition range, and the copper-zinc alloys

have been investigated more completely than almost any other alloy series in the field of physical metallurgy, the single property of stacking fault energy is alone unique at this composition. The stacking fault energy for the 25 w/o zinc alloy is considerably lower than that for alloys containing more or less zinc.

Since the material response to a hardness test which is sensitive to grain boundaries is necessarily plastic, attention must be directed to the manner by which dislocation shear passes from one crystal to the next through the grain boundary. It has been found that such passage involves a change in both the area and the angular dimension of the grain boundary. Each of the two crystals must participate so as to remain coherent as the dimension change occurs. Simple dislocations arriving at the grain boundary result in a shape change in the contributing grain which must be matched by a corresponding shape change by the generation and transmission of new dislocations in the receiving grain.

When stacking faults occur the dislocations are split into partials that travel separately across the

crystal plane. A partial dislocation arriving at the grain boundary results in only an elastic deformation at the boundary, until its matching component arrives. Thus in the presence of stacking faults, there is introduced an elastic resistance superimposed on the resistance of plastic flow of the dislocation into the boundary. The lower the stacking fault energy, the greater the separation of the halves of the split dislocations, and the more prominent is the elastic component of the resistance to plastic deformation. Thereby, a low stacking fault energy for the 25 w/o zinc alloy leads to a high intercrystalline boundary hardening effect.

A more detailed analysis of this process must begin with a more complete consideration of the nature of the deformation that takes place in indentation hardness testing.

4.10 Indentation Hardness Measurements on Alpha Brass

To better explain hardness measurements, they will first be analyzed at a given alloy composition.

4.11 Hardness at a Given Composition

In the present research, it has been shown that the relationship between Brinell hardness and intercrystalline boundary area provides a method whereby the hardness contributions of the crystal and crystal boundaries can be separated. Although the intercrystalline boundary contribution to hardness is really to be associated with simply a change in deformation across the interface, for discussion purposes, this phenomenon will be referred to as the intercrystalline boundary contribution to hardness per se. In other words, in this discussion, a polycrystal's hardness will be divided into parts, one part relating to the average crystal hardness $(BHN)_o$, and the other part relating to the crystal boundary contribution to hardness $(BHN)_B$. Therefore, if a normal polycrystalline hardness number was determined at a given value of boundary area, suppose 2000 cm^2/cm^3, and expressed as $(BHN)_P$, an equation relating these measurements would be:

$$(BHN)_P = (BHN)_o + (BHN)_B \qquad (1)$$

Although these two parts, $(BHN)_o$ and $(BHN)_B$, constitute the total of a polycrystal's hardness, they do not by themselves give any information about the various elastic and plastic responses of the test material.

Harris (1922) introduced the strainless hardness number $(BHN)_s$, which measures a true elastic limit, or in other words, an elastic response per se. Since a normal hardness number is composed of both an elastic and plastic response, the plastic response $(BHN)_w$ could be obtained by subtracting the elastic response $(BHN)_s$ from a normal hardness number. The plastic response $(BHN)_w$ is also referred to as the strain hardening contribution to a hardness number. It it is assumed that Harris's (1922) strainless hardness $(BHN)_s$ is a finite part of $(BHN)_p$, and thus a finite part of both $(BHN)_o$ and $(BHN)_B$, equation (1) could be expanded to give:

$$(BHN)_P = (BHN)_o + (BHN)_B = \left[(BHN)_s\right]_o + \left[(BHN)_s\right]_B + \left[(BHN)_w\right]_B + \left[(BHN)_w\right]_o \qquad (2)$$

where:

$\left[(BHN)_s\right]_o$ = an average true elastic limit of a crystal

$\left[(BHN)_s\right]_B$ = an average true elastic limit of a crystal boundary

$\left[(BHN)_w\right]_o$ = an average strain hardening contribution of a crystal

$\left[(BHN)_w\right]_B$ = an average strain hardening contribution of a crystal boundary

Equation (2) expresses a straight forward approach to the crystal and crystal boundary response to elastic and plastic deformation where it is assumed that both provide a finite and distinguishable resistance to deformation. In alpha brass, it appears that the elastic response of the material is completely independent of crystal size. Intuitively, the reason for such a condition is that the elastic properties of alpha brass are isotropic and therefore have no sensitivity to crystal boundaries, which are seen only as differences in crystal orientation, while the plastic properties are anisotropic (sensitive to crystal planes) and therefore feel the orientation differences at crystal boundaries.

Some support for such thoughts is found in common stress versus strain curves from polycrystalline materials. For instance, if several specimens of 70-30 copper-zinc were tested in tension, and each specimen had a different grain size, the resulting stress-strain curves would be

similar to those shown in Figure 19. The stress-strain curves shown in Figure 19 were taken from Holloman (1945). During the early stage of deformation, when all of the specimens are truly elastic, the curves lie on top of one another showing that the effect of grain size is negligible. Larger strains induce plastic deformation whereupon the material of finer grain size displays more resistance to deformation. The result of all this is that $[(BHN)_s]_b \approx 0$, which reduces equation (2) to equation (3):

$$(BHN)_P = (BHN)_o + (BHN)_B = [(BHN)_s]_o + [(BHN)_w]_o + [(BHN)_w]_B \quad (3)$$

This information is shown schematically in Figure 20, where Brinell hardness is plotted as a function of boundary area for any given composition of alpha brass.

The result that the elastic response of the grain boundary $[(BHN)_s]_B$ is negligible in the deformation of polycrystalline aggregates leads to two important conclusions: (1) the magnitude of the strainless hardness $(BHN)_s$ remains almost the same at all values of boundary area (or grain size), and (2) the contribution of the crystal boundary to the magnitude of a hardness number depends upon an interaction between plastic deformation and the crystal boundary.

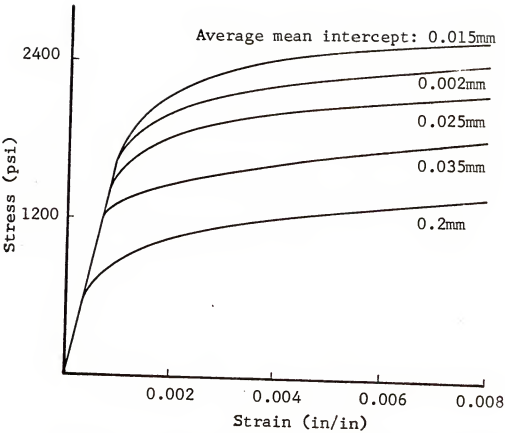

Figure 19. Tensile stress versus strain curves for different grain size specimens of 70-30 copper-zinc. Taken from the investigation of Hollomon (1945).

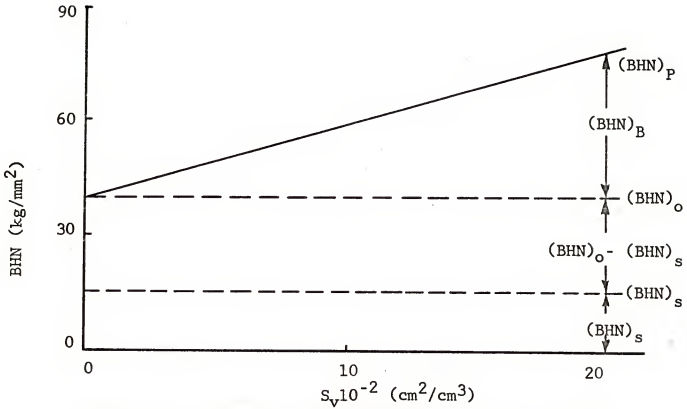

Figure 20. Schematic representation of the strainless, average crystal, and boundary area hardness contributions that make up a polycrystalline hardness number

4.12 Hardness as a Function of Composition

Indentation hardness measurements obtained from fine grained polycrystalline alloys of alpha brass show a pronounced hardness maximum at approximately the 25 w/o zinc composition. In order to analyze this maximum in hardness, it is necessary to plot polycrystalline hardness $(BHN)_p$, average crystal hardness $(BHN)_o$, and Harris's (1922) strainless hardness $(BHN)_s$ on a single set of axes. These hardnesses are all shown in Figure 21 where Harris's (1922) strainless hardness $(BHN)_s$ (the lower relationship), average crystal hardness $(BHN)_o$ (the middle relationship), and finally the polycrystalline hardness at a constant boundary area of 2000 cm^2/cm^3, are plotted as a function of zinc concentration in alpha brass. $(BHN)_s$ is a measure of the true elastic limit and therefore comprises only part of a normal hardness number. $(BHN)_o$ is a measure of the true elastic limit plus the strain hardening contribution of the hardness number of an average aggregate grain (without crystal boundaries). $(BHN)_p$ is a measure of the true elastic limit and the strain hardening contribution to the hardness number of an average aggregate grain and a specified area of intercrystalline boundary area. Note that, as a

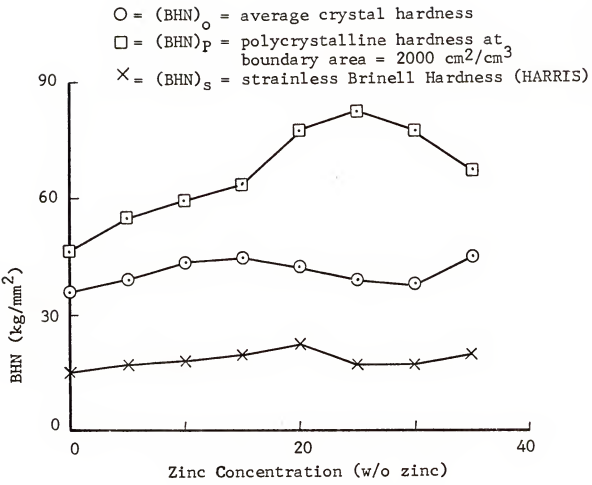

Figure 21. A comparison of Harris's (1922) strain hardness, average crystal hardness, and polycrystalline hardness as a function of zinc concentration in alpha brass

function of composition, the $(BHN)_s$ and $(BHN)_o$ measurements are separated by a relatively constant hardness number, whereas $(BHN)_p$ shows an irregular separation when compared to either $(BHN)_s$ or $(BHN)_o$. The increase of $(BHN)_p$ above $(BHN)_o$ is the hardness contribution of the boundary area per se. Thus, it is the boundary area contribution to hardness that produces the maximum in the polycrystalline hardness number at 25 w/o zinc. Since the total elastic response of the material (crystal and crystal boundary) is contained in $(BHN)_s$, any part that is above this measurement is to be associated with plastic deformation. Still further, since $(BHN)_o$ is regularly related to $(BHN)_s$ while $(BHN)_p$ is irregular to both $(BHN)_s$ and $(BHN)_o$, the polycrystalline hardness maximum is to be associated with an interaction between intercrystalline boundaries and plastic deformation per se.

4.20 Dislocations in Plastically Deformed Alpha Brass

The current metallurgical literature shows that alpha brass is subject to stacking faults, which are planar regions that separate pairs of partial dislocations. When

the energy required to produce a stacking fault is small, the partial dislocations, one at each edge of the stacking fault, may be spread far apart. The energy for the stacking fault formation (called stacking fault energy) has in general been found to diminish rapidly with zinc content throughout a large portion of the composition range of alpha brass, and in fact, the recent measurements of Thomas (1963) show a pronounced minimum of approximately 25 w/o zinc, Figure 22.

Alpha brass has also been found subject to short range ordering. The occurrence of such ordering begins at zinc concentrations of about 20 w/o zinc and increases quadratically to the limit of the alpha field at about 39 w/o zinc. Although Keating (1954) suspected the existence of long range ordering at 25 A/o zinc, and a critical temperature of 95°C, Köster and Schüle (1957) and Clarebrough, Hargreaves, and Loretto (1961) have not been able to confirm this suspicion.

The existence of short range order tends to increase the stacking fault energy at alpha brass compositions with zinc contents higher than 30 w/o zinc.

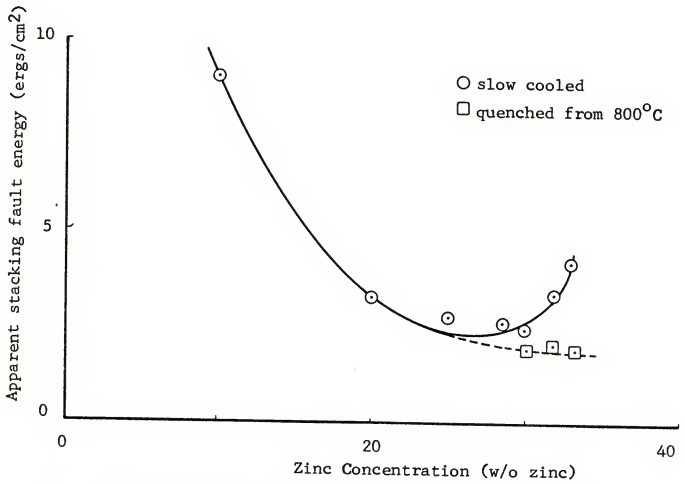

Figure 22. Apparent stacking fault energies versus zinc concentration in slow cooled and quenched alpha brass alloys, Thomas (1963)

Thomas (1963) explains that the minimum in stacking fault energy is to be associated with a reversal of the trend to lower fault energy at higher zinc contents as the counter effect of short range ordering that becomes significant at about this composition. Although Thomas (1963) has been able to show a correlation between atomic order and stacking fault energy, he has not speculated on the interaction mechanism. The writer suggests that one possibility is an interaction of the leading partial dislocation with short range order which causes the stacking fault regions to become narrower. This type of idea was previously expressed by Fisher (1954) and Flinn (1960), for the interaction of total dislocations with zones of atomic ordering, and most certainly is applicable to the partial dislocation-atomic ordering interaction. Thus, the more order present, the narrower the faults, and correspondingly the higher the stacking fault energy.

Verification of the dependence of stacking fault widths upon alloy composition in alpha brass is found in the investigations of Swann and Nutting (1962), Thomas (1963), and Bell, Roser, and Thomas (1964). They show

that stacking fault widths and three-dimensional dislocation arrangements can be separated into three distinct regions: (1) from pure copper out to about 20 w/o zinc they find very narrow or non-existent stacking faults arranged in the form of cellular networks, (2) from 20 to 30 w/o zinc, the stacking faults are wide, coplanar, and tend to pile up, and (3) above 30 w/o zinc, the faults are narrower and coplanar, the dislocations exist in pairs, and extensive cross-slip is observed near any existing pile ups. Thus, in terms of a single mechanism, such as cross-slip, the observations are: (1) extensive cross-slip from copper to about 20 w/o zinc, (2) little or no cross-slip between 20 and 30 w/o zinc, and (3) the return of cross-slip above 30 w/o zinc. Cross-slip is directly related to stacking fault widths in that the partial dislocations must recombine to a total dislocation in order to cross-slip.

4.30 Intercrystalline Boundary-Shear Dislocation Interaction in Alpha Brass

Since it has been established that the hardness maximum found for fine grained alpha brass alloys at 25 w/o zinc is to be associated with an interaction between

intercrystalline boundaries and plastic deformation, and that partial dislocations show the widest separation at this same composition, a thorough analysis of the dislocation-intercrystalline boundary interaction is in order.

The intercrystalline boundary-shear dislocation interaction has been introduced using the model of Rhines (1965). In relation to the present investigation, there are several ideas presented in this model that bear further consideration. For instance, in the alpha brasses it is found that: (1) the resistance to plastic deformation that is associated with an intercrystalline boundary is derived from the fact that slip planes in conjoint grains are not parallel, (2) no matter what the atomic mechanism of the dislocation-intercrystalline boundary interaction, the resistance to plastic deformation that is felt at the boundary is in proportion to the two-dimensional area of the interface, and (3) a plastically deformed intercrystalline boundary shows an increase in two-dimensional area that is proportional to the burgers vector of each dislocation and the number of dislocations that intersect the boundary per unit area.

Whenever a dislocation intersects an intercrystalline boundary, the slip planes in the conjoint grain are non-coincident. This is shown schematically in Figure 23, where the grain boundary has been hypothetically removed from the bicrystal shown in Figure 38, Appendix V. The slip planes from conjoint grains are theoretically traced along the interface, showing the problem of shear transmittal between grains. Since the grains on each side of the interface must remain contiguous, the accomodation problem at the interface forces the shear steps along the interface to be as uniformly small as is physically possible within the limitations of the available slip planes. For instance, a large step (multiple slip on a single slip plane) along the interface would not be possible without causing a fissure or crack. In fact, it was pointed out long ago by Von Mises (1928) that in order for crystals to remain contiguous along the intercrystalline boundaries during plastic deformation, a minimum of five slip systems must be operative.

Alpha brass is known to slip on a multiplicity of slip planes. Thus, whenever a dislocation arrives at

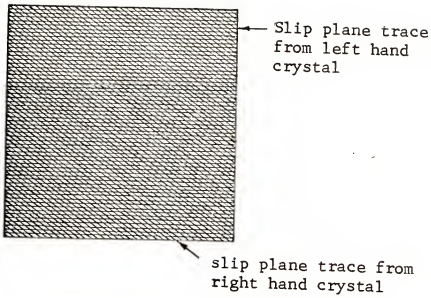

Figure 23. Schematic of an intercrystalline boundary showing slip plane traces from conjoint crystals

an intercrystalline boundary, it can either intersect the boundary or possibly cross-slip. Therefore, if the dislocation could cross-slip, the dislocation-intercrystalline boundary intersections would be spread out over the available surface area. This condition would tend to minimize the accommodation problems along the interface.

It is also known that dislocations in alpha brass separate into partial dislocations. Each total dislocation separates into two partials that form a stacking fault region along the slip plane. It is impossible for a single partial dislocation to cross-slip. Thus, whenever a partial dislocation approaches an intercrystalline boundary, it is forced to remain on its slip plane until the stacking fault region is removed by the recombination of the partial dislocations. Whenever the partials are recombined, the total dislocation can then cross-slip. Therefore, to evenly spread out the deformation along the intercrystalline boundary when the dislocations are broken into partial dislocations, the partials must be recombined and the stacking fault regions eliminated before the dislocation intersects the intercrystalline boundary. Probably the best way to

characterize this process would be to consider that the partial dislocation feels an elastic resistance at the intercrystalline boundary that repulses the partial dislocation, forcing the partials to recombine as a penultimate step to plastically deforming the intercrystalline boundary.

To quantitatively estimate the energy required to eliminate the stacking fault regions per unit volume of material, information is needed about the fault width per dislocation line, the specific fault energy and the per cent of the total slip planes that are faulted. The specific fault energies were taken from the node measurements of Thomas (1963). Stacking fault energy is related to the fault width per dislocation line through a relationship introduced by Cottrell (1953), i.e., $r = \mu a^2/24\pi\gamma$, where r = partial dislocation separation, μ = shear modulus, a = atomic spacing, and γ = stacking fault energy. Stacking fault probability is related to stacking fault energy through the equation $\alpha = A\epsilon^2/\gamma$, where α = stacking fault probability, A = constant, ϵ^2 = mean square strain obtained from X-ray analyses of peak shifts, and γ = stacking

fault energy. It has been experimentally confirmed that in alpha brass, stacking fault energy can be used to estimate stacking fault widths and stacking fault probabilities, or vice versa.

To compare the fault energy per unit volume of material for different compositions of alpha brass, the fault width per slip plane (r) is considered on a unit length basis. Thus, the area of fault per slip plane would be r(1). Since the fault energy per unit area is known, the energy per fault could be expressed as $r(1)\gamma$. It must also be remembered that as a function of composition each unit volume of material is not faulted on the same percentage of slip planes. The fault energy per unit volume of material is therefore $r(1)\gamma\alpha$, where $r = K/\gamma$, and $\alpha = K'/\gamma$. The parameters K and K' are $\mu a^2/24\pi$ and $A\epsilon^2$ respectively. Including the expressions for r and α reduces the equation for the fault energy per unit volume of material to $(1)KK'/\gamma$. To simplify calculations, a ratio technique is adopted using copper as the ratio base. By doing this the parameters (1)KK' are eliminated, and the relationship becomes $(1/\gamma \text{alloy})/(1/\gamma \text{copper})$. This ratio,

which reduces to $\gamma_{copper}/\gamma_{alloy}$, is a measure of the energy required to eliminate all of the stacking faults per unit volume of alloy material divided by the energy required to eliminate the stacking faults in copper. With this ratio technique, the numbers have a common base starting with the ratio number one for copper to copper. This information is summarized in Table XII .

Hardness measurements can also be expressed in terms of the energy required to deform a unit volume of material, Chattergee (1956). It is shown in Appendix IV that measurements of Brinell hardness and the energy necessary for the deformation of a unit volume of material are equivalent throughout the alpha brasses. Thus, the slope of the Brinell hardness-boundary area relationship, which is a measure of the hardness contribution of intercrystalline boundaries per se, is also a measure of the energy required to deform intercrystalline boundaries. To give these measurements a common base for subsequent comparisons, a ratio technique is adopted where all alloy energies for boundary deformation are divided by equivalent measurements for pure copper.

TABLE XII

Stacking Fault Energies, Stacking Fault Energy Ratios, and the Boundary Area Contribution to Hardness Ratios for Alpha Brass

Alloy	γ* (ergs/cm^2)	$\frac{\gamma \text{ copper}}{\gamma \text{ alloy}}$	$\frac{(\Delta \text{BHN}/\Delta S_v) \text{ alloy}}{(\Delta \text{BHN}/\Delta S_v) \text{ copper}}$
100	12.2	1.00	1.00
95-5	9.3	1.31	1.46
90-10	7.0	1.74	1.54
85-15	4.8	2.54	1.82
80-20	3.4	3.58	2.48
75-25	2.9	4.20	4.21
70-30	2.7	4.52	3.74
65-35	5.0	2.44	2.08

*Stacking fault node measurements of Thomas (1963).

A comparison of the fault energy per unit volume of material (the circles) and the energy necessary to deform the intercrystalline boundaries (the x's) is shown in Figure 24 where the dimensionless ratios mentioned above are plotted as a function of zinc concentration in alpha brass. Certainly the most outstanding result shown in Figure 24 is that both dimensionless ratios are a maximum at approximately 25 w/o zinc. It is therefore concluded that stacking faults must be eliminated as a penultimate step to the plastic deformation of intercrystalline boundaries.

At the outset of the present reserach, the purpose was to find out what specific feature caused the maximum hardness for certain fine grained alloys of alpha brass. It has been shown that the hardness maximum for alloys of approximately the 25 w/o zinc composition depends explicitly upon the shear dislocation-intercrystalline boundary interaction and the energetics of the specific interaction at each composition. For compositions near 25 w/o zinc, the shear dislocations are separated into wide stacking faults that must be eliminated as a penultimate step to the plastic

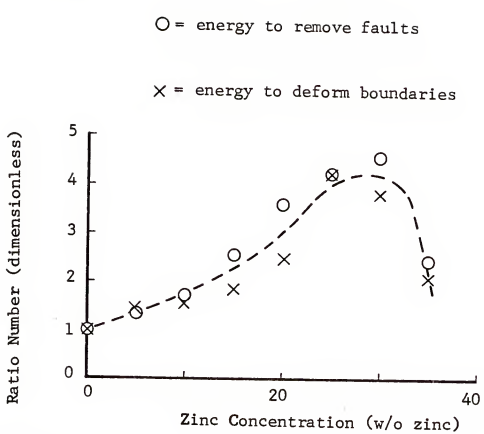

Figure 24. Comparison of the energy required to deform intercrystalline boundaries and remove stacking faults in alloys of alpha brass divided by similar measurements in pure copper

deformation of the intercrystalline boundary. The additional energy required to eliminate the stacking faults, which is a maximum at approximately 25 w/o zinc, is identically equal to the additional deformation energy measured by the intercrystalline boundary area contribution to hardness. Since the crystal contribution to hardness per se is about the same at all alloy compositions, the maximum hardness for fine grained alloys near the 25 w/o zinc compositions is thus explained as an intercrystalline boundary contribution to hardness.

Further verification of the composition dependence of the dislocation-intercrystalline boundary interaction is obtained from: (1) quenching experiments, and (2) the temperature survey.

4.31 Quenching Experiments

The decrease in the boundary area contribution to hardness that was found for alloys beyond the 30 w/o zinc composition of alpha brass was explained by the effect of short range order upon dislocation geometry (stacking fault widths) and subsequently the resulting dislocation-grain boundary interaction. A series of tests was devised to check the dependence of this interaction upon short range

order. Atomic ordering can be "quenched out" by a rapid quench into iced brine from approximately 873°K. Clarebrough, Hargreaves, and Loretto (1961) studied the kinetics of the ordering process, showing that after quenching, the high zinc content alpha brasses require about two hours standing at room temperature for reordering. Following this information, alloy composition of 70-30, 67-33 and 65-35 copper-zinc were tested using a variety of different quenching solutions, specimen sizes, and quenching temperatures. This survey is the subject of Appendix VII, and the writer will limit the current discussion to the specific results that pertain to the boundary area contribution to hardness.

Quenched and slow-cooled specimens, when compared at each alloy composition showed: (1) the same boundary area hardness contributions at 70-30 copper-zinc, (2) a slight difference, but not really much change for the 67-33 copper-zinc alloy, and (3) a definite increase in the hardness contribution of the boundary area for the quenched specimens at 65-35 copper-zinc. If these same specimens were then aged at room temperature for one week or longer,

a comparison of the "as quenched" and the "quenched and aged" state showed: (1) no change for the 70-30 copper-zinc composition, (2) very little change for the 67-33 alloy, and (3) a definite decrease in the boundary area hardness contribution for the quenched and aged 65-35 alloy. Therefore, the results of this survey show that by eliminating short range order at 65-35 copper-zinc, the boundary area hardness contribution is increased to a contribution that is very near the 75-25 copper-zinc composition maximum, but with the return of short range order, the boundary area hardness contribution is decreased towards its normal value.

More evidence that the high zinc content alloys of alpha brass contain short range order, and that this ordering effects mechanical properties was found by the author in a compressive stress versus strain analysis made at seven compositions spanning the alpha brasses, Appendix III. The evidence was, that at several per cent strain and above, the stress versus strain relationships for the high zinc content alloys were jerky and serrated. Serrated stress-strain curves have long been explained

by the interaction of plastic deformation and atomic order. This effect was found only at the compositions where substantial amounts of short range order was suspected, 30 w/o zinc and above.

4.32 Temperature Dependence

The grain boundary area contribution to hardness at compositions near 25 w/o zinc have been shown to decrease rapidly with increasing temperature. At 573°K, the maximum boundary area hardness contribution was significantly decreased, but still could be called a maximum, while at 373°K the maximum was non-existent, and in fact, it had become a minimum.

The negative slope found for the hardness versus boundary area relationships near the compositions of 25 w/o zinc at 873°K implies that at this temperature, the intercrystalline boundaries no longer act as barriers to plastic deformation. This thought does not agree with the model or interpretation presented for the lower temperature hardness measurements. Therefore, the writer decided to check the high temperature results by measuring impact hardness on copper and 70-30 copper-zinc as a function of boundary area

and temperature. These experiments were conducted in part by Rhode (1967), and they are presented in fullin his senior thesis. The results that are directly related to the present investigation are shown in Figure 25, parts (a) and (b). Part (a) shows the impact hardness versus boundary area relationships at 298 and 873°K for pure copper, whereas part (b) shows the same relationships for 70-30 copper-zinc. The important result of the tests is that at rapid test rates (where the complete test time is less than 1/8000 second) the hardness contribution of intercrystalline boundary area is unchanged from 298 to 873°K. Thus, by eliminating diffusion mechanisms, the contribution of boundary area to hardness is retained even at 873°K.

Swann and Nutting (1962) have shown that in alpha brass, the stacking faults disappear with increasing temperature. The temperature range where the faults disappear is also the range where the boundary area hardness maximum disappears. Thus, at high temperature, if the test rate is slow enough the faults diffuse away and do not interfere whereas at fast strain rates this does not happen. Therefore diffusion readily explains the decreasing boundary

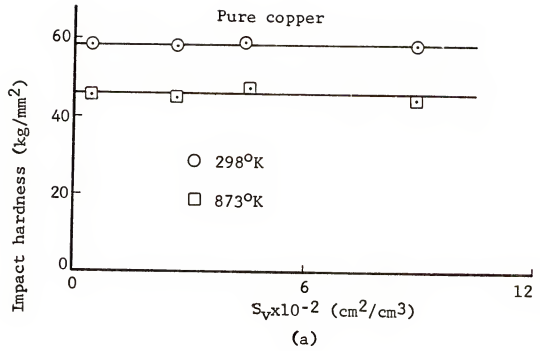

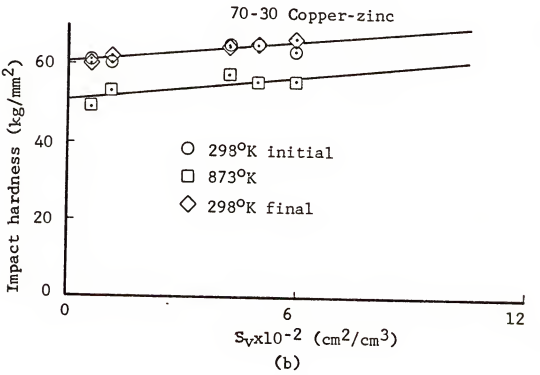

Figure 25. Impact hardness versus boundary area for pure copper and 70-30 copper-zinc at 298 and 873°K

area contribution to hardness maximum with increasing temperature at about 25 w/o zinc, but does not explain the minimum at 873°K.

Grain boundary shearing is one possible explanation for the regular decrease in hardness found with increasing boundary area at 873°K. Although grain boundary shearing is not completely understood, it has long been recognized as important in mechanical property measurements at high temperatures. It seems reasonable to assume that if the intercrystalline boundaries were subject to shearing, an extra degree of freedom would be added to the deformation process at the intercrystalline boundaries which would therefore decrease the boundary contribution to hardness per se.

Other investigators have also recognized that there is something special about the alpha brasses with compositions near 25 w/o zinc at high temperatures. For instance, Feltham and Copley (1959) studied creep behavior on polycrystalline alloys of alpha brass showing a maximum activation energy and a maximum creep rate for the 25-30

w/o zinc alloy compositions. Also, Sherby (1962),(1967) has empirically related creep rates measured on polycrystalline alloys of alpha brass to an equation that includes stacking fault energy. It has been established by Atkins, Silverio, and Tabor (1966) that Brinell testing is an acceptable method for studying creep rates.

The various studies of the hardness-boundary area relationships also provide information about the average crystal hardness as a function of both composition and temperature.

4.40 Average Crystal Hardness in Alpha Brass

The dependence of average crystal hardness upon alloy composition and test temperature will be considered separately.

4.41 Composition Dependence

The average crystal hardness of alpha brass was found to be relatively insensitive to alloy composition. The small change of average crystal hardness with composition at any one of the test temperatures implies that

the solute zinc has little hardening effect on the solvent copper. It is generally recognized that the hardness of solid solutions depends upon the relative atomic sizes of the solvent and solute with the amount of hardening afforded by the solute increasing with increasing atom size difference. Copper and zinc, being elements 29 and 30 in the periodic series, have very similar atomic radii. Therefore, it is not surprising that the average crystal hardness of alpha brass is relatively insensitive to zinc content.

The form of the relationships between average crystal hardness and composition was found to remain almost the same at all test temperatures. At lower temperatures the relationships show a slow increase of average crystal hardness with increasing zinc content out to about 15 to 20 w/o zinc, a shallow minimum between 20 and 30 w/o zinc, and an increase at 35 w/o zinc. These relationships were shown in Figure 10 where the average crystal hardness was plotted as a function of zinc concentration in alpha brass. The shape of these relationships relates directly to the dislocation-dislocation intersections within the crystals. For instance, at compositions from copper to about 20 w/o

zinc the dislocations cross-slip and tangle causing the crystal to harden simply by flow restrictions. From 20 to 30 w/o zinc the dislocations are strongly restricted to slip planes and form a non-intersecting network of dislocations on parallel slip planes, as was shown by Suzuki (1965) and coworkers. Thus, at these compositions, there are very few dislocation-dislocation intersections which results in a lower crystal hardness that is minimum where the dislocations are most restricted to slip planes (25 w/o zinc). Beyond 30 w/o zinc cross-slip returns and the flow restrictions from dislocation-dislocation interactions again produce an increase in the crystal hardness.

It is also important to note that the low temperature average crystal hardnesses show a definite increase where short range order is expected to be important (35 w/o zinc) whereas at high temperature, where short range order is absent, there is a decrease in hardness.

4.4.2 Temperature Dependence

The average crystal hardness versus composition relationships show a regular decrease with increasing

temperature, Figure 10. The metallurgical literature provided very little information on mechanical properties over the temperature range currently studied. This was especially true when seeking information on single crystals. The only complete set of property measurements available over this composition and temperature range were contained in the investigation of Köster (1940), who measured the dynamic elastic moduli of the alpha brasses from 298 to 973°K. His measurements were made on large grain size specimens by determining the fundamental resonant frequency of rectangular specimens during transverse "free-free" vibration. These measurements show a regular behavior with increasing temperature at all alpha brass compositions.

A comparison of the per cent decrease of average crystal hardness with increasing temperature shows a direct correspondence to the per cent decrease in elastic modulus over the same temperature interval. These measurements are summarized for the 95-5, 85-15, 72-28, and 67-33 copper-zinc alloys at the test temperatures of 298, 573, and 873°K in Table XIII. Also, relative comparisons of the per cent change in average crystal hardness and elastic modulus

TABLE XIII

Dynamic Elastic Modulus Measurements of Köster (1940) and Average Crystal Hardness for 95-5, 85-15, 72-28, and 67-33 Copper-Zinc at 298, 573, and 873°K

Elastic Modulus (E)$\times 10^{-3}$ (kg/mm^2) (Köster)				
	95-5	85-15	72-28	67-33
298°K	13.0	12.4	11.5	11.3
573°K	11.8	11.1	10.2	10.1
873°K	9.5	8.8	7.9	7.2
Average Grain Hardness $(BHN)_o$ (kg/mm^2)				
298°K	39.8	44.9	38.6	42.5
573°K	36.5	40.4	36.5	40.0
873°K	27.1	31.8	28.5	23.0

from 298 to 573°K and 298 to 873°K are shown as a function of alloy composition in Figure 26. In general, at each alpha brass composition, the per cent change in these measurements is seen to be similar. This correspondence implies that the decrease in average crystal hardness with increasing test temperature is for the most part a result of a decrease in the elastic portion of the hardness measurements. A second implication is that the strain hardening part of the hardness measurement remains fairly constant at all test temperatures.

Some sense of the reasonableness of these results is obtained by analyzing the mechanics of a Brinell test at high test temperatures. Observation of a high temperature hardness test reveals that the indenter moves into the test material at a fairly rapid rate. Thus, at elevated temperature the strain rate of the material under the indenter is much higher than at low temperature. In general, this would tend to increase the strain sensitivity of the material, or appear as a lower temperature result. Granted, the elastic modulus must be assumed to be fairly strain rate insensitive, but the metallurgical literature shows

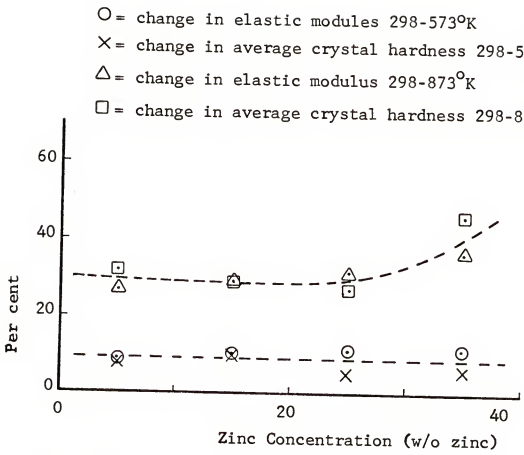

Figure 26. Per cent change of elastic modulus and average crystal hardness from 298-573°K and 298-873°K as a function of zinc concentration in alpha brass

that this is not such a bad assumption. Thus, the decrease in average crystal hardness with increasing temperature can be at least qualitatively attributed to an equivalent percentage decrease in the elastic response of the test material.

4.43 Comparisons of Average Crystal Micro- and Macrohardness

At the outset of the present investigation, some doubt was attached to the validity of the average crystal hardness measurement. The extrapolations of the hardness-boundary area relationships, used to obtain average crystal hardnesses, are less than 5 per cent of the coordinate axes, but since extrapolation beyond any measured region often raises doubts, experiments were devised to cross check the average crystal hardness measurements. This was done by placing microhardness impressions in the center of twenty-five grains at each alloy composition. Average crystal Brinell hardness $(BHN)_o$ and average grain center microhardness $(DPN)_o$ are separately plotted as a function of zinc concentration in alpha brass in Figure 27, parts (a) and (b). The similarity of these two relationships, and the relative magnitudes of the hardness numbers obtained

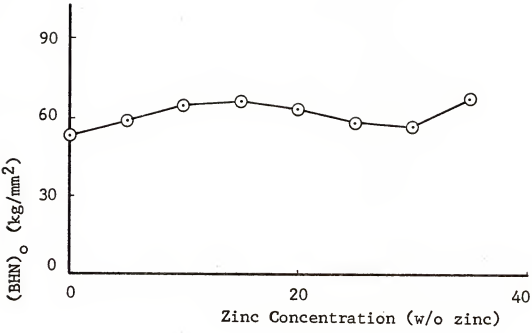

(a)

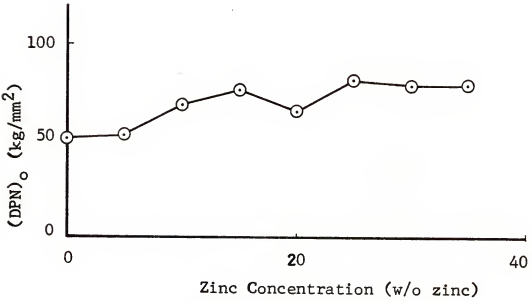

Figure 27. (a) Average crystal Brinell hardness versus zinc concentration for alpha brass
(b) Average crystal microhardness versus zinc concentration for alpha brass

in each case convinced the writer that the average crystal hardness measurements are valid.

The average crystal microhardness measurements were only part of several surveys conducted during the course of the present investigation. Although the information obtained in these surveys is of a supplemental nature, some rather unique and interesting comparisons are brought out.

4.50 Meyer Analysis

A Meyer analysis, which is normally used to determine the so called pretest hardness $(MHN)_K$, and the strain hardening coefficient (n)were used in the present research to: (1) make a conversion of Brinell hardness to energy per unit volume of deformation through the method of Chattergee, Appendix IV, (2) analyze strain hardening and its relation to intercrystalline boundaries, and (3) determine hardness numbers at various stages of plastic deformation so that comparisons could be made with tensile stress-strain measurements.

4.51 Meyer Pretest Hardness and Tensile Yield Points

The Meyer pretest hardness $(MHN)_K$ is not a normal indentation hardness measurement in that it is determined at a constant indentation surface area. Pretest hardness is measured at a very early stage of plastic deformation by sampling the load versus impression diameter relationships determined in the Meyer analysis at an impression diameter of one millimeter. Because of this sampling method, wherein hypothetical hardness numbers are determined that are representative of a test that is still in progress, the writer considers the pretest hardness as a dynamic rather than static type hardness measurement. It is of course true that yield points are measured by a similar sampling technique.

Tensile yield points were obtained, at a constant intercrystalline boundary area of 800 cm^2/cm^3, from the investigation of Feltham and Copley (1960). Feltham and Copley's (1960) yield point measurements were made on completely recrystallized alloys of alpha brass, and provided an ideal series for comparisons with the pretest hardness. In order to make comparisons, the Meyer pretest hardness versus intercrystalline boundary area relationships

shown in Figure 13 were sampled at a boundary area of 800 cm^2/cm^3. It should be added that Feltham and Copley (1960) defined their yield points as the stresses at which deviations from the stress-strain curve in the elastic range first became apparent.

Meyer's pretest hardness and tensile yield points are compared as a function of zinc concentration in alpha brass in Figure 28, parts (a) and (b). The shapes of these relationships are very similar, with the pretest hardness being approximately 6.5 times larger than the yield points at all alloy compositions. It is important to note that neither measurement shows anything special about the 25 w/o zinc alloy composition.

It is implied from the correspondence of these measurements that the pretest hardness and yield point (as defined) both measure a load or stress per support area ratio that is characteristic of a very early stage of the plastic deformation process. Still further, since it has been shown that the Meyer pretest hardness relates on unknown amounts of plastic deformation, the same situation is suggested for the yield point measurement.

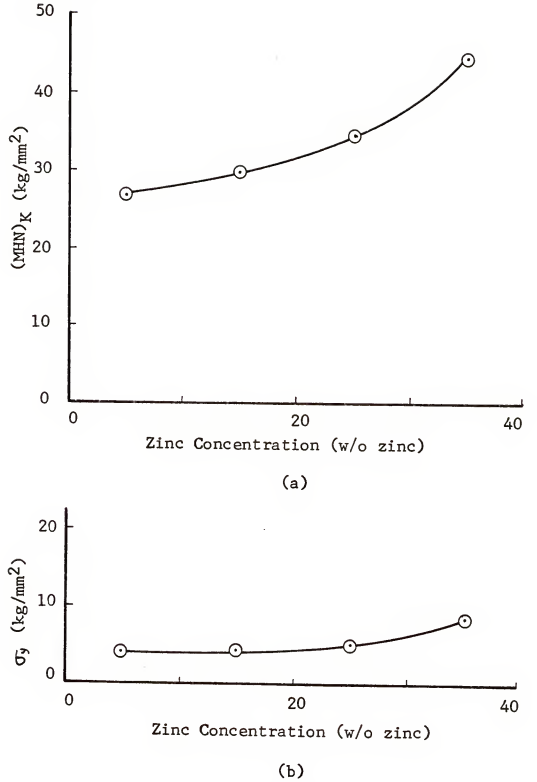

Figure 28. (a) Meyer pretest hardness versus zinc concentration in alpha brass
(b) Feltham and Copley's (1960) tensile yield points versus zinc concentration in alpha brass

From the comparisons mentioned above, the writer can find no justification for the general assumption by other investigators that yield points and normal Brinell Hardness Numbers should be related. Thus, it is not surprising to find that the composition dependence of the relationship between Meyer pretest hardness and intercrystalline boundary area does not show a direct correspondence with the composition dependence of the normal hardness-boundary area relationships.

4.52 Meyer Strain Hardening Coefficients

Meyer strain hardening coefficients are easily obtained and have been the subject of several previous investigations. However, until recently, very little importance has been placed on the possibility of intercrystalline boundaries having more than a negligible effect upon these measurements. The present Meyer strain hardening coefficient versus intercrystalline boundary area relationships show a small but regular dependence of the strain hardening coefficient upon boundary area for all alpha brass alloys, Figure 14. If the various relationships for

different alloy compositions shown in Figure 14 are compared as a function of boundary area, it is interesting to note that at low boundary area the coefficient is smallest for the 25 w/o zinc alloy, whereas at high boundary area the coefficient is largest for the 25 w/o zinc alloy. Interest was therefore generated in the validity of these measurements.

Strain hardening coefficients of a qualitative nature were available for large and small values of boundary area in the tensile stress-strain analyses of Feltham and Copley (1960) and Argent, Blank, and Nissen (1965). These coefficients were taken from the linear part of the plastic portion of the stress-strain curves. Since these measurements could only be roughly interpreted, subsequent comparisons will show trends, and no special significance should be attached to the numbers involved.

Meyer strain hardening coefficients and tensile deformation strain hardening coefficients are plotted as a function of zinc concentration in alpha brass for low boundary area specimens in Figure 29, parts (a) and (b). Note that both relationships show a minimum at 25 w/o

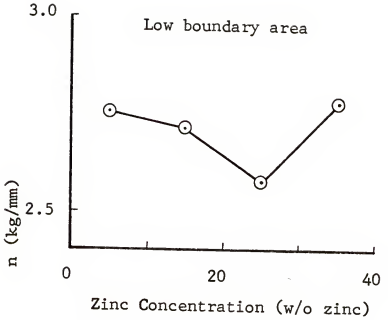

(a)

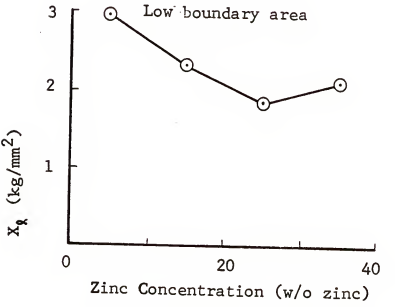

(b)

Figure 29. (a) Meyer strain hardening coefficient versus zinc concentration in alpha brass
(b) Feltham and Copley's (1960) linear strain hardening coefficient versus zinc concentration in alpha brass

zinc. Similar measurements are plotted for high boundary area specimens in Figure 30, parts (a) and (b). Note that both of these relationships show a maximum at 25 w/o zinc. It is thereby concluded, that in relation to the dependence of strain hardening coefficient-intercrystalline boundary area measurements upon composition the Meyer strain hardening coefficients are valid measurements.

The result that strain hardening coefficients are highest for the 25 w/o zinc alloy at high boundary area and lowest at low boundary area, agrees with the general hardness versus boundary area analyses. For the 25 w/o zinc alloy in comparison to the other alloys, strain hardening coefficients imply that at low boundary area there is more plastic deformation per unit of load (a low hardness number), whereas at high boundary area there is less plastic deformation per unit of load (a high hardness number.). This is indeed the experimental result found for the hardness measurements on the 25 w/o zinc alloy, i.e., in comparison to the other alloys, the 25 w/o zinc alloy is softest when the grain size is large, and hardest when the grain size is small.

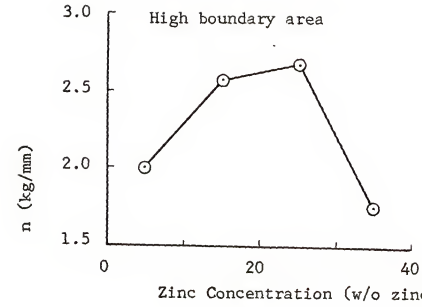

(a)

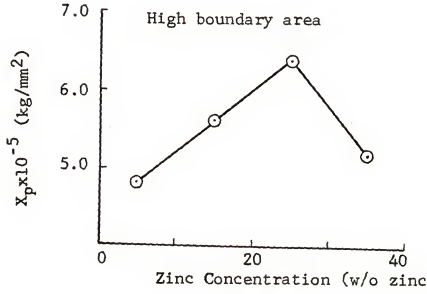

(b)

Figure 30. (a) Meyer strain hardening coefficient versus zinc concentration in alpha brass
(b) Feltham and Copley's (1960) parabolic strain hardening coefficient versus zinc concentration in alpha brass

4.53 Meyer Strain Sensitivity Limit of Boundary Area

It has long been known that alpha brass alloys in the composition range of 25-30 w/o zinc can be used for deep drawing applications whereas other alloy compositions can not. For a metal to deep draw, it must remain plastic over an extremely wide range of reduction. In general, this requires that the metal deform uniformly throughout the deformation process.

The strain sensitivity limit of boundary area $(MHN)_L$, that is obtained from the Meyer analysis, shows that the intercrystalline boundaries of the 25 w/o zinc alpha brass alloy composition remain sensitive to plastic deformation at much higher percentages of deformation than the other alloys. The writer interprets the long range sensitivity of intercrystalline boundaries at 25 w/o zinc to the fact that plastic shear is strongly restricted to parallel slip planes, which minimizes the dislocation-dislocation interactions that tend to excessively harden the crystals. Therefore, the present research indicates that the metallic property of deep drawing, that is the outstanding characteristic of cartridge brass (30 w/o zinc) depends upon the fact that this alloy deforms uniformly on

parallel slip systems that do not grossly interact, whereas in contrast, the other alloy compositions deform inhomogeneously by dislocations that profusely cross-slip, produce tangles, and finally cause the deformed metal to fissure at locally hardened regions.

4.60 Vickers Microhardness

Westbrook and Wood (1963), Mott (1956), and many other investigators have studied grain boundary properties using microhardness. For the most part, the measurements are extremely time consuming and must be limited to a given set of conditions, as for instance a bicrystal. Some microhardness investigations have been conducted on intermetallics wherein the intercrystalline boundaries are found to give a much higher microhardness than the surrounding grains. Such is not the case for phase pure materials such as alpha brass, and in fact, Mott (1956) mentions that microhardness measurements from intercrystalline boundaries of single phase materials are only a few per cent greater than grain center microhardnesses.

4.61 Microhardness Measurements on Recrystallized Alpha Brass

The alpha brasses presently investigated have shown that a comparison of the average microhardness from grain centers and grain boundaries bears out Mott's (1956) statement. The intercrystalline boundaries are approximately 3-4 per cent higher in microhardness at all alpha brass compositions.

The similarity of the grain center and intercrystalline boundary microhardness measurements at all compositions of alpha brass brings out an important point. The hardness contribution of the intercrystalline boundaries obtained from the Brinell measurements must result from an interaction of grains that are totally constrained within the polycrystalline aggregate.

In the microhardness test, the multiple slip systems of alpha brass cause the deformation that is induced in a local zone along the test surface to take the easiest path. The easiest path is plastic flow within the crystal as opposed to plastic flow from crystal to crystal through the crystal boundary.

4.62 Microhardness Measurements on Prestrained Alpha Brass

Takamura and SeiMiura (1959) measured grain and grain boundary microhardnesses on prestrained bicrystals of alpha brass showing that the boundary region was much harder. Attempts were made to measure this effect on prestrained polycrystals of alpha brass by measuring a large number of grain center and grain boundary microhardnesses at each alloy composition. The experimental scatter was so large that no definite conclusions could be drawn about grain versus grain boundary microhardnesses.

In general, it is therefore concluded that the microhardness technique is a very limited tool for the study of grain boundary properties in polycrystals of single phase alloys such as alpha brass.

4.70 Investigation of Alpha Silver-Zinc

Brinell hardness was measured as a function of intercrystalline boundary area and temperature for the 20, 25, and 30 A/o zinc alloys of alpha silver-zinc. This survey was initiated by the author to check the generality

of the results obtained from the alpha copper-zinc alloys and was conducted by Jenkins (1967). All measurements were made following the investigation on copper-zinc.

4.71 Brinell Hardness versus Intercrystalline Boundary Area

Brinell Hardness Number was found to be directly proportional to the intercrystalline boundary area for the alpha silver-zinc alloy compositons of 20, 25, and 30 A/o zinc at the test temperatures of 77 and 298°K, Figures 31 to 33.

4.72 Average Crystal Hardness

Average crystal hardness is plotted as a function of zinc concentration in alpha silver-zinc in Figure 34. At 77°K, the average crystal hardness shows a small but steady increase with increasing zinc content, whereas at 298°K, the average crystal hardness is decreased in magnitude but remains almost constant as a function of composition.

A comparison of the average crystal hardness-composition relationships for silver-zinc, Figure 34, and similar measurements for copper-zinc, Figure 10, shows a

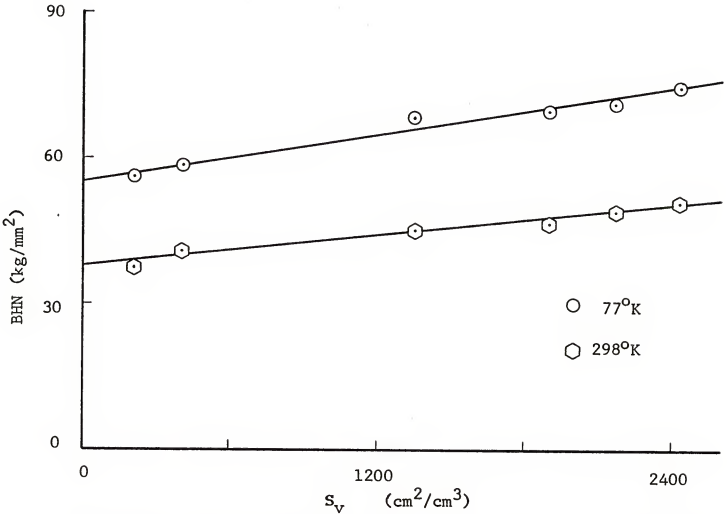

Figure 31. Brinell Hardness Number versus boundary area per unit volume for 19.8 A/o zinc alpha silver-zinc

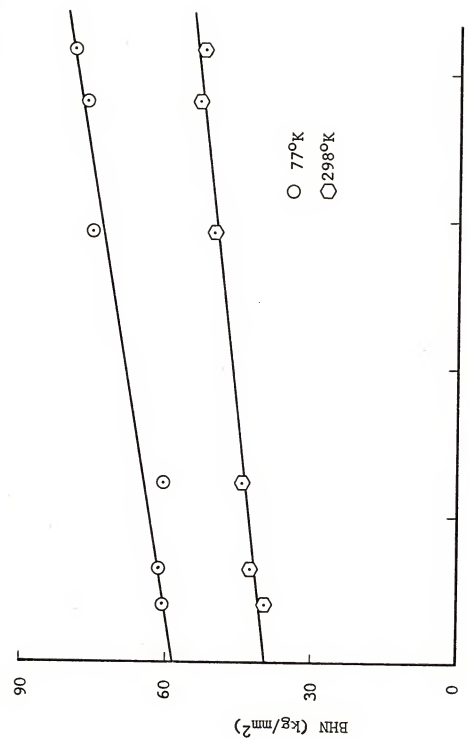

Figure 32. Brinell Hardness Number versus boundary area per unit volume for 25 A/o zinc in alpha silver-zinc

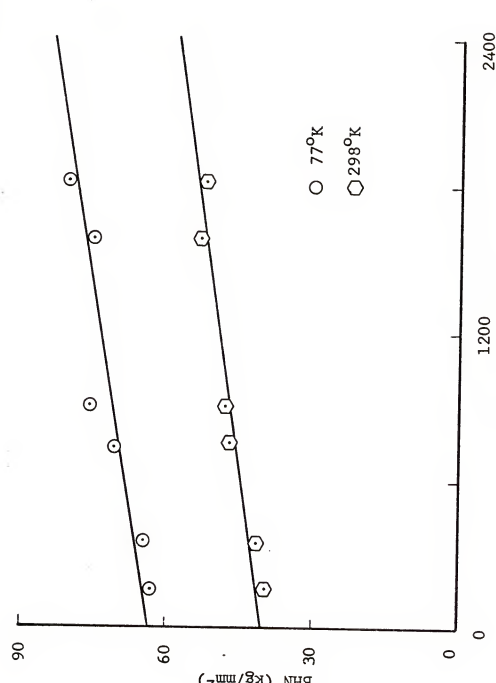

Figure 33. Brinell Hardness Number versus boundary area per unit volume for 29.2 A/o zinc in alpha silver-zinc

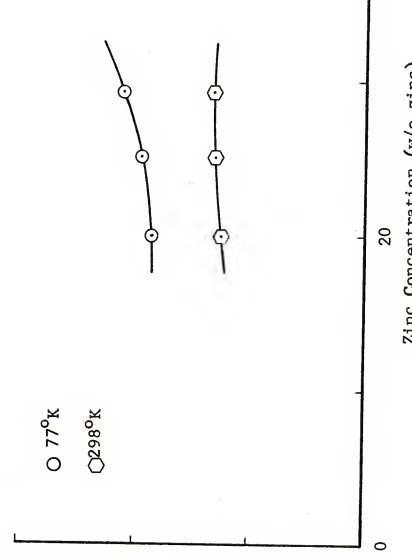

Figure 34. Average crystal hardness versus zinc concentration in alpha silver-zinc

direct correspondence. The dependence of this relationship upon test temperature seems to be shifted to a lower temperature in alpha silver-zinc. For instance, 77°K for silver-zinc is equivalent to either 77 or 298°K in copper-zinc whereas 298°K in silver-zinc corresponds to a temperature somewhere between 573 and 873°K in copper-zinc.

4.73 Boundary Area Contributions to Hardness

The relationships determined from the plot of boundary area contribution to hardness versus zinc concentration in alpha silver-zinc, Figure 35, also shows a definite similarity to the corresponding plots of alpha copper-zinc, Figure 11. The low temperature measurements on both alloys show a maximum at approximately 25 A/o zinc whereas at higher test temperatures, a minimum is found at the same composition. Once again the temperature dependence of hardness is found to become important at much lower temperatures in alpha silver-zinc.

Nowick (1952) offers one possible explanation for the low temperature decay of hardness measurements in alpha silver-zinc when he showed that diffusion rates of zinc in

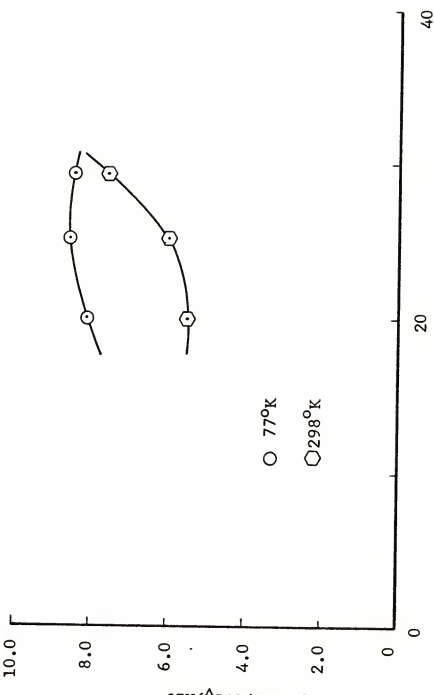

Figure 35. Boundary area contribution to hardness versus zinc concentration in alpha silver-zinc

silver are five times greater than in copper. Nowick's (1952) measurements were suggested to be applicable at 298°K. Thus, it is not surprising to find that the absolute magnitude of the boundary area contribution to hardness are smaller, and that the dependence of hardness upon test temperature show a shift to lower temperature for the silver-zinc alloys.

It is proposed for the correspondence of the various measurements obtained from the alpha silver and copper-zinc alloys, that if stacking fault energy measurements were made using the technique of Thomas (1963) a minimum stacking fault energy would be found at approximately 25 A/o zinc in silver.

CHAPTER V

CONCLUSIONS

From the present research it can be concluded that:

1. The Brinell Hardness Numbers obtained from recrystallized alloys of alpha brass (0-35 w/o zinc) are directly proportional to the intercrystalline boundary area per unit volume at the test temperatures of 77, 298, 573, and 873°K.
2. Of the many crystal dimension measurements available for explaining property-grain size relationships, the intercrystalline boundary area is the most accurate crystal dimension measurement available for correlation with indentation hardness.
3. The relationship between Brinell hardness and intercrystalline boundary area provides a method for the separation of the fundamental hardness of the crystal from the hardness contribution of the intercrystalline boundary.

4. The fundamental hardness of the crystal is relatively insensitive to alloy composition in alpha brass.
5. The intercrystalline boundary contribution to hardness is strongly sensitive to alloy composition showing a pronounced maximum at the 25 w/o zinc alloy composition.
6. The intercrystalline boundary contribution to hardness measures the energy to pass plastic deformation (as distinguished from elastic deformation) from one crystal to the next through the intercrystalline boundary.
7. Plastic shear dislocations in alpha brass are subject to the formation of stacking faults, and these faults are widest at the 25 w/o zinc alloy composition.
8. The decrease of stacking fault widths beyond the 25-30 w/o zinc alloy compositions results from glide restrictions produced by an interaction of stacking faults and short range order.
9. The interaction of plastic shear dislocations and intercrystalline boundaries forces stacking faults to be eliminated as a penultimate step to the plastic deformation of the intercrystalline boundary.

10. The additional energy that must be provided to eliminate the wide stacking faults for alloys near 25 w/o zinc is equivalent to the extra energy measured in the intercrystalline boundary area contribution to hardness maximum at this same composition.
11. The decay of the intercrystalline boundary contribution to hardness with increasing test temperature results from the elimination of stacking faults by diffusion mechanisms.
12. The analogous experimental results obtained from the alpha silver-zinc alloys show that the present investigation techniques are not restricted to a single alloy system.

CHAPTER VI

SUGGESTED RESEARCH

The present research on alpha copper and silver zinc suggests several new areas for continued investigations. These are:

1. Brinell Hardness Number as a function of intercrystalline boundary area and composition in the alpha copper-aluminum and copper-tin alloy systems. These alloy systems have ideal alpha solubility ranges for isolating and studying the dependence of the hardness-intercrystalline boundary interaction upon stacking fault energy without the side effects of short range order. The alpha solubilities are narrow enough such that there is no short range order, but wide enough to cause a stacking fault energy decrease comparable to alpha copper-zinc. Stacking fault energies are known, the alloys are workable, and direct comparisons of experimental data with the known data on alpha copper-zinc might help to better understand the relationship between hardness-boundary area, stacking

fault energy, and short range ordering. The conclusions drawn from the present investigation indicate that a future investigator could expect a steady increase in the intercrystalline boundary contribution to hardness with increasing solute content in both alloy systems.

2. Brinell Hardness Number as a function of intercrystalline boundary area, composition, and temperature in the copper-gold alloy system. This alloy system offers a wide variety of possibilities for investigation. A hardness versus boundary area survey, made at composition intervals of 12.5 A/o, and at test temperatures from 77°K to above one-half of the alloys' melting point, would represent "lots of work" but also "lots of information." The effects of long range order upon the hardness-boundary area relationship, if any effects are found, could be studied at the 1:3, 1:1, and 3:1 atomic order ratios. Both ordered and disordered states could be studied at the same compositions through the temperature survey, or possibly by naturally cooled versus quenched specimen conditions.

Information available in the metallurgical literature suggests that long range order increases the contri-

bution of grain boundaries to mechanical properties. In general this thought is in agreement with the present copper-zinc investigation, except that in the ordered copper-gold alloys the dislocation geometry consists of total dislocations separated by a stacking fault, rather than the partial dislocations-stacking fault arrangement found in alpha copper-zinc. In both cases it seems reasonable that the stacking fault would be eliminated during the dislocation-grain boundary interaction step of plastic deformation. Therefore both dislocation-stacking fault arrangements should cause a high dislocation-grain boundary interaction energy. Since the backlog of information available in the literature on copper-gold is voluminous, little more need be said.

3. The relationship between two-dimensional mean intercept ($\overline{\lambda}$) and three-dimensional mean grain diameter ($\overline{D_V}$) in alpha brass. This type of investigation would require serial sectioning, or sampling the grain structure throughout its physical dimensions. A microtome could be used to accurately slice away known amounts of metal from a polycrystalline specimen, with the two-dimensional grain

boundary network being recorded at predetermined intervals by photomicrographs. These two-dimensional micrographs could then be used to construct the true three-dimensional grain shapes and to analyze possible relationships between the various measurements of quantitative metallography. Other investigators have supposed that three-dimensional grain diameter can be measured on a single slice through an equiaxed polycrystalline array of grains, whereas the present theorems of quantitative metallography say that this is not so. In any case, if there is a correlation, it should be pointed out in its true meaning.

An ideal system for this investigation from the standpoint of easy grain size preparation, cutting on the microtome, electropolishing, and etching would be 70-30 copper-zinc. The only problem encountered at the outset would be the annealing twins.

4. Meyer strain hardening coefficients, from the center of large polycrystalline grains, measured by microhardness. To conduct microhardness experiments on strain hardening, it would be necessary to rig up a very small spherical indenter for the microhardness tester. With careful application of the spherical indenter at a series

of different small loads, it would be possible to determine strain hardening coefficients from within separate polycrystalline grains. To facilitate these measurements, hardness impressions at different loads could be made one after another in the same location. Previous investigators claim that the error introduced by such an operation as this is trivial. This same test would then be repeated on several grains, and at alpha brass compositions of 95-5, 85-15, 75-25 and 65-35 copper-zinc. Conclusions drawn in the present research indicate that the strain hardening coefficient of an average aggregate grain should be relatively independent of alloy composition. The microhardness measurements would provide a direct comparison. Also, if the micro-indenter was small enough, the same type of experiment could be repeated at two grain sizes at each alloy composition. These experiments would provide a second check on a conclusion obtained from the present research, that is, that the strain hardening in an average polycrystalline aggregate grain is relatively independent of grain size in alpha brass.

5. It is suggested that, in all future studies of hardness as a function of intercrystalline boundary area, the primary series of hardness measurements be made using at least three different loads. The reason for this is that the information gained would be more than tripled for the same amount of time expended. Also, a better comparison could be made with previous investigations, several different indenter to specimen contact angles would be established, and the Meyer analysis information could be analyzed.

APPENDICES

APPENDIX I

AVERAGE PRESSURE DERIVATION

O'Neill (1934), Tabor (1951), and other investigators have expressed dissatisfaction with the Brinell Hardness Number because they do not believe it is based on a satisfactory physical concept. The reason for this is that the ratio of the load to the curved area of indentation does not give the mean pressure over the surface of indentation. To show this, it is assumed that the mean pressure is given as P, that there is no friction between the indenter surface and the indentation, and that the pressure acts normal to the surface of the indentation, Figure 36. Consider the forces on a curved annulus of radius with width ds. The area of the annulus lying on the curved surface of the indentation is $2\pi x ds$ and the force of it is $P(2\pi x ds)$. The horizontal component of this force, by symmetry considerations, is zero. The vertical component is $P(2\pi x dx)$. If a sum is taken over the whole surface area of the indentation, the resultant

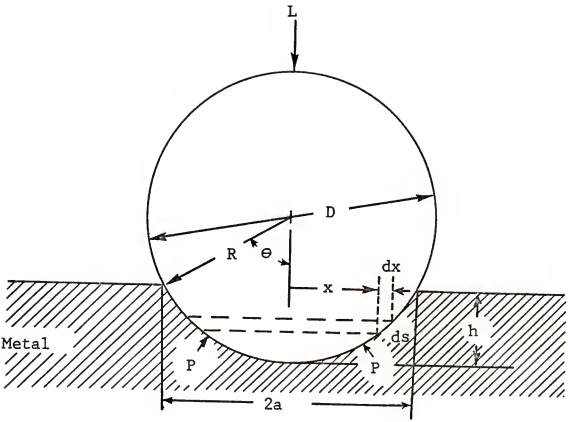

Figure 36. Schematic of the indenter and indentation dimensions related to a hardness test using a spherical ball

horizontal force, as expected is zero. The resultant vertical force which is equal to the normal load is simply:

$$L = \int_0^a P2\pi x dx = P\pi a^2$$

where 2a is the chordal diameter of the indentation. Consequently, the mean pressure is equal to $L/\pi a^2$.

Thus the mean pressure between the surface of the indenter and the indentation is equal to the ratio of the load to the projected area of the indentation. This quantity as a measure of the hardness was first proposed by Meyer (1908). The Meyer Hardness Number is expressed as:

$$MHN = 4L/\pi d^2$$

where $d = 2a$.

APPENDIX II

CORRELATIONS OF MECHANICAL PROPERTIES AND GRAIN SIZE

Considerable attention has been given to the problem of calculating the flow stress, or yield point in metallic polycrystalline aggregates. Taylor in his classical theory of 1938, proposed that polycrystal properties are only a sum of single crystal properties, i.e., he used the result that continuity between polycrystalline grains determines the deformation process within the grain and so determines the stress required for deformation. Taylor's (1938) calculations have been generalized by Bishop and Hill (1951), Hill (1952), and Kocks (1958), with all of these theories predicting polycrystalline properties as simple multiples of single crystals.

Hall (1951) and Petch (1953) introduced a concept and derivation wherein they attempt to explain the effects of polycrystalline grain size upon lower yield points, as in iron and steel, and flow stresses, as in non-ferrous

metals and alloys. Petch's (1953) derived equation was $\sigma_f = \sigma_o + kl^{-1/2}$, where σ_f = the flow stress or yield point at constant strain, σ_o = a constant representing the friction stress of an isolated dislocation on a slip plane, and $kl^{-1/2}$ = the additional stress that must be added to σ_o in deforming a polycrystalline material. The term k is taken to be a constant for a given material under a given set of test conditions and l is the so called "grain diameter" that is measured on a two-dimensional section. The original derivation of this equation depends upon the stress conditions at the leading edge or tip of an existing crack or fissure as introduced by Griffith's (1920). The Griffith (1920) crack theory is applied by making the assumptions that: (1) a grain boundary is a barrier to dislocation flow, (2) dislocations pile up along the slip plane causing a concentrated stress to be applied to the lead dislocation, and (3) the stress concentration factor is proportional to the number of dislocations in the pile. The result of this theory is the equation expressed above which says that the stress necessary to push a dislocation in proportional to the square root of the reciprocal of the "grain diameter."

Armstrong et al. (1962) mention the application of Petch's (1953) theory to several alloys of alpha brass. Flow stress was found to be directly proportional to the negative square root of the "grain diameter" at any constant value of strain up to 20 per cent. Most of the investigations on brass were conducted by Meakin, and were fully presented by Meakin and Petch (1962). It should be mentioned that the "grain diameter" measurement used by Petch and coworkers becomes even more confusing in brass because of the annealing twins. These twins are always considered in the "grain diameter" measurement.

Numerous investigations on a variety of metals and alloys, e.g., Cracknell and Petch (1955), Codd and Petch (1960), Adams and Higgins (1959), Johnson (1959), (1960), Churchman (1960), Adams et al. (1960), and others, have shown that the Petch equations holds over a wide range of grain size. However, recently, several questions have been raised about the validity of the basic mechanism, the pile ups, and also about the true meaning of "grain diameter." Measurements made on a plane

section cannot measure three-dimensional grain diamter in a polycrystalline aggregate as shown by Desch (1919), Hull and Houk (1953) and Smith and Guttman (1953). Rhines and Lemons (1968) have also expressed concern over the general acceptance of "grain diameter." Therefore, although the equation of Petch (1953) seems to hold in a variety of situations, there exists a fundamental problem in that the theory and experimental measurements are not considering the same parameter.

Over the past few years, there has been a running discussion of what polycrystalline aggregate dimension best explains the yield strength data. In general, most of the measurements are actually related to the surface area of the crystal boundaries or some function of the boundary area. It is also true that most of these measurements are a function of, or proportional to the two-dimensional mean intercept ($\bar{\lambda}$). It usually follows, that if the units of the so called "grain diameter" measurements (ℓ) or (d) are made similar, they are numerically equal to $\bar{\lambda}$. This has not always been the case, but in the more recent "grain diameter" measurements by counting

methods such as intercept counting with known length test line, $\bar{\lambda} = d = \ell$. Therefore, the functions that are most commonly used to explain yield strength data can be expressed as $(\bar{\lambda})^{-n}$ where n can take on the values of 1, 1/2, or 1/3. The groups identified with $(\bar{\lambda})^{-1}$ are supposedly followers of Bragg (1942), who first introduced this concept. Kocks (1967) also contends that $(\lambda)^{-1}$ is the correct parameter, but he interprets its meaning in terms of average distance that a dislocation travels along a slip plane in a three-dimensional grain without intersecting an obstacle. Wood (1930) and followers who use x-ray techniques to measure grain size also claim that $(\bar{\lambda})^{-1}$ is the correct measurement, but they interpret $(\bar{\lambda})^{-1}$ in terms of the interfacial boundary area. It is of course true that $(\bar{\lambda})^{-1} = 2N_L = S_V$, and therefore the relationship does expand directly into a measurement of the boundary area per unit volume (S_V). The parameter $(\bar{\lambda})^{-1/2}$ is the Hall-Petch interpretation and $(\bar{\lambda})^{-1/3}$ was introduced by Baldwin (1958). Baldwin (1958) showed that most any of the known yield strength data gave a straight line relationship when plotted versus $(\bar{\lambda})^{-n}$ where

n was 1, 1/2 or 1/3. Baldwin (1958) liked the 1/3 power because the extrapolations of the yield strength versus $(\bar{\lambda})^{-1/3}$ relationships went to zero at infinite $\bar{\lambda}$. Kocks (1959) and others were quick to point out that the extrapolation through zero was physically meaningless.

Since these various measurements find common application to metallurgical problems, the writer decided to check what power of n from $(\bar{\lambda})^n$ best fit the hardness data obtained from recrystallized copper-zinc. A Model 709 IBM computer was programmed for a best fit index to the above mentioned relationships.[1] The best fit was $(\bar{\lambda})^{-1}$, or the hardness versus boundary area relationships presented in the body of this thesis.

Another challenge to the Hall-Petch theory has been expressed by Conrad (1961), (1963), and Meakin and Petch (1962). The new analysis of grain and grain boundary restrictions to dislocation flow depends upon experimental results obtained through electron transmission microscopy. This theory uses the variation in dislocation

---

[1]Courtesy of J.H. Steele.

density with grain size and the interaction of moving dislocations with the long-range internal stress fields that are associated with dislocations already present throughout the grain matrix per se. This theory has also found many proponents, e.g., Conrad and Christ (1963), Conrad (1963), Marcinkowski and Fisher (1965), Dingley and McLean (1967), and Conrad, Feuerstein, and Rice (1968). This theory sort of bridges the gap between several schools of thought in that the basis goes all the way back to Taylor (1938) and the resulting formula used to explain flow stress is qualitatively interpretable in terms of the Hall-Petch analysis. One interesting point made in this theory, is that grain boundaries act as nucleation sites for new dislocations. Thus, the number of dislocations present in the polycrystal grains depends upon the grain size. Quantitative estimates of the number of dislocations within strained polycrystalline grains as a function of grain size are not yet available, but investigations are supposedly in progress. This theory could possibly agree in some respects with the present investigations. Before any correlations could be

attempted, it would be necessary to know if the number of dislocations nucleated at grain boundaries are directly related to grain boundary area,or some other parameter.

APPENDIX III

COMPRESSIVE STRESS-STRAIN ANALYSIS

Brinell Hardness Number, engineering yield strength, and ultimate tensile strength, have often been empirically related. Interest was thereby generated in an investigation on alpha brass wherein yield strength would be determined as a function of boundary area. The supplies of base materials had dwindled, so the writer decided to conduct a limited survey with the materials available. This later proved to be a mistake because the range of boundary area sampled was much too narrow. The narrow boundary area range precluded any comprehensive comparisons with the hardness survey, but the problems encountered will be mentioned in hopes that some time might be saved for future investigators.

In order to establish a comparable range of grain size at each alpha brass alloy composition, the following procedure was followed: (1) choose a 1 1/4 inch cube at each alloy composition (each cube had a similar uniform recrystallized grain size), (2) cut each cube into 5/8 x

5/8 x 5/8 x 1 1/4 inch pieces, (3) cold roll three of the four pieces at each composition varying amounts along the 5/8 inch square faces, (4) heat treat and cold work these same three specimens at each composition in order to produce a different uniform grain size in each specimen, and (5) polish, etch, and measure all specimens for intercrystalline boundary area. The alloys were then prepared for mechanical testing by: (1) machining each piece into a 1/4 x 3/4 inch cylinder on a metal lathe (the last step was to face the specimen ends in order to produce parallel loading surfaces), (2) chemically remove all of the tool marks with a nitric acid solution, and (3) give all specimens a final heat treatment at 500°C for fifteen minutes.

Compression testing was done using an Instron testing machine, a strain rate of 10^{-2} in/in per minute, and a 3 mil teflon sheet at each end of the specimen to reduce friction. Finally, stress versus strain relationships were calculated from the data. Four types of information were taken from these diagrams: (1) the stress at the first deviation from the linear or Hookian behavior at the beginning of deformation ($\sigma_{E.L.}$), (2) the stress at a

constant strain of 0.05 mm/mm (σ_5), this value was used because some yield drop type of behavior was found in some of the alloys causing stresses at earlier values of strain to be a little confusing, (3) the area under the stress-strain curve from zero to a predetermined value of strain, and (4) the slope of the linear portion of plastic deformation (n_{II}), or the so called strain hardening coefficient during Stage II determinations. All of this information is summarized in Table XIV.

The problems encountered in this research were: (1) the loading surfaces at each end of the specimens were not parallel enough, (2) the boundary area range sampled was too narrow (150-650 cm^2/cm^3), and (3) the specimens were too small. Possible solutions to these problems are: (1) the new helical loading device available from Instron for compression testing, or a lapping arrangement for making the specimen ends perfectly parallel, (2) more material, and (3) the specimens should have at least twenty grains in a cross section at the largest grain size tested, the general width to length ratio is 1:3.

TABLE XIV

Measurements Taken from Compressive Stress versus Strain Experiments on Recrystallized Alpha Brass

Alloy	S_V (cm^2/cm^3)	$\sigma_{E.L.}$ (kg/mm^2)	σ_5 (kg/mm^2)	Area (kg/mm^2 - mm/mm)	n_π (kg/mm^2 - mm/mm)
95-A	221.3				
95-B	389.4	0.526	1.300	0.519	20.53
95-C	262.4	0.730	1.342	0.541	22.00
95-D	313.1	1.159	1.609	0.686	17.63
90-A	354.1	0.758	1.725	0.675	26.03
90-B	477.9	0.634	1.441	0.570	22.34
90-C	514.3	0.552	1.378	0.557	23.30
90-D	309.8	0.548	1.370	0.553	22.40
85-A	291.1	0.826	1.610	0.638	23.71
85-B	437.8	0.673	1.387	0.562	25.21
85-C	312.5	0.638	1.392	0.554	25.37
85-D	303.7	0.643	1.355	0.552	24.58
80-A	630.4	0.776	1.497	0.583	26.10
80-B	414.5	0.644	1.425	0.556	26.09
80-C	545.6	0.644	1.380	0.553	25.29
80-D	267.8	0.640	1.325	0.540	24.94
75-A	451.1	0.705	1.365	0.559	24.40
75-B	355.8	0.778	1.360	0.565	23.41
75-C	222.5	0.644	1.240	0.506	22.98
75-D	231.5	0.606	1.240	0.514	22.85
70-A	255.2	0.734	1.400	0.566	21.80
70-B	340.6	0.917	1.422	0.603	22.70
70-C	227.6	0.666	1.262	0.528	22.23
70-D	138.2	0.620	1.240	0.462	21.98

TABLE XIV (Continued)

Alloy	S_v (cm^2/cm^3)	$\sigma_{E.L.}$ (kg/mm^2)	σ_5 (kg/mm^2)	Area (kg/mm^2 - mm/mm)	n_T (kg/mm^2 - mm/mm)
65-A	417.1				
65-B	301.2	0.751	1.275	0.527	21.94
65-C	187.4	0.698	1.192	0.493	23.55
65-D	155.2	0.688	1.259	0.524	21.35

APPENDIX IV

HARDNESS AND ENERGY PER UNIT VOLUME

Chattergee (1956) introduced the following method for converting Brinell Hardness Numbers to the energy required per unit volume of material deformation. Referring to Figure 36 of Appendix I:

A vertical load is applied to a spherical indenter of diameter D creating an indentation of chordal diameter 2a or d and depth h. The work done, W, is then given by:

$$W = \int_{o}^{h} Ldh \qquad (4)$$

Since L is not independent of h, the Meyer law is used to establish a relationship,

$$L = kd^{n} \qquad (5)$$

$$K = A/D^{n-2} \qquad (6)$$

where A and n are constant, depending on the nature of the material but independent of the ball diameter D. From Figure 36 it is obvious that,

$h = R(1 - \cos\theta)$

$d = 2R \sin\theta$

substituting into equation (4)

$$W = A\, 2^3\, R^3\, (1/2) \int_0^{\theta} \sin^{n+1}\theta \, d\theta \qquad (7)$$

In equation (7), the indentation angle θ and index n are both variables and n in general is not an integer. Suppose that

$$1/2 \int_0^{\theta} \sin^{n+1}\theta \, d\theta = F(n) \qquad (8)$$

where F(n) is some function of n for a given value of θ. If $F(\theta)$ and $G(\theta)$ are two independent functions of θ, then

$$\int_0^{\theta} F(\theta)\, G(\theta)\, d\theta \Big/ \int_0^{\theta} F(\theta) d\theta = f(\theta) \qquad (9)$$

where $f(\theta)$ is another function of θ defined by equation (9). Substituting $\sin^{n+1}\theta$ for $F(\theta)$ and $\ln \sin\theta$ for $G(\theta)$ gives

$$1/2 \int_0^{\theta} \sin^{n+1}\theta \, \ell n \sin\theta \, d\theta = f(\theta)\ 1/2 \int_0^{\theta} \sin^{n+1}\theta \, d\theta \tag{10}$$

From equation (8) it is obvious that

$$\frac{d\,F(n)}{dn} = 1/2 \int_0^{\theta} \sin^{n+1}\theta \ \ell n \sin\theta \, d\theta \tag{11}$$

combining equations (8), (10), and (11) gives

$$\frac{d\,F(n)}{dn} = f(\theta)\ F(n) \tag{12}$$

$$\text{let} \quad \beta = f(\theta) \tag{13}$$

$$\text{then} \quad F(n) = \alpha e^{\beta n} \tag{14}$$

Note that β is a function of θ but independent of n. Hence, for a given value of θ, β can be taken as constant independent of the nature of the material. Combining equations (7), (8), and (14) gives

$$W = A2^3\ R^3 \alpha e^{\beta n}$$

From Figure 36, the volume of the indentation is given by

$$V = \frac{\pi h^3}{3}(3R-h) = \frac{\pi R^3}{3}\left[\,2-\cos\theta\,(\sin^2\theta+2)\right]$$

The hardness H defined as W/V is therefore given by

$$H = W/V = \frac{A\ 24 \propto e^{\beta n}}{\pi[2-\cos\theta\ (\sin^{-2}\theta + 2)]}$$

$$= \frac{K(24D^{n-2} \propto e^{\beta n})}{\pi[2-\cos\theta\ (\sin^{2}\theta + 2)]} \qquad (15)$$

Therefore, with a known contact angle, and the information from the Meyer analysis, it is possible to calculate the energy required to deform a unit volume of material.

Chattergee (1956) shows that a normal Brinell Hardness Number, and the Hardness Number (H) expressed in equation (15) are similar for several materials.

The author decided to use the information gathered in the Meyer analysis to check this relationship for the presently studied alpha brasses. Although the Meyer analysis is "not the best" in the current investigation, the Brinell Hardness Numbers and the energy required to deform a unit volume of material were very close for all of the alloys tested. This information is summarized in Table XV.

TABLE XV

Information for the Calculation of the Energy Required to Deform a Unit Volume of Material by the Method of Chattergee (1956)

Specimen	S_v (cm^2/cm^3)	n (kg/mm)	k (kg)	H=E/v (kg/mm^2)
95-2	226.9	2.734	11.14	39.29
95-14	361.5	2.525	17.21	45.09
95-11	494.5	2.617	15.62	46.99
95-3	759.3	2.455	20.42	48.76
95-7	766.2	2.498	19.17	48.67
95-4	1205.0	2.282	29.29	55.00
85-2	183.9	2.666	13.81	44.33
85-3	310.9	2.608	16.72	49.36
85-10	646.3	2.527	19.92	52.66
85-6	821.1	2.504	22.02	56.27
85-3	1562.5	2.253	35.88	64.76
75-2	278.4	2.544	15.08	40.70
75-11	374.8	2.534	20.05	53.44
75-10	491.0	2.433	22.00	50.93
75-3	1033.1	2.310	34.30	67.84
75-4	1454.0	2.317	38.02	75.04
25-2	265.8	2.617	14.58	43.74
25-10	364.8	2.534	19.62	52.02
25-15	501.8	2.350	28.00	57.80
25-6	731.7	2.305	29.40	58.09

Characterization of A Brinell Hardness Test

A normal Brinell hardness test on a normal polycrystalline metal is far from simple. Therefore, the writer will spell out a series of events that could be used to characterize the various stages of the indentation process and the resulting material states at each stage. For the sake of explanation, three different situations will be evaluated and compared. For instance: (1) a normal metal but a special hardness test (the load applied to the indenter is adjustable); (2) a special metal (where no strain hardening takes place during plastic deformation) and a normal hardness test; and (3) a normal metal and a normal hardness test.

Situation (1): At any load, when the indenter first touches the test surface, the metal is elastically distorted such that if the indenter were immediately removed, no permanent indentation would remain. There is no easy way to measure the amount of elastic distortion of this early stage of deformation. This is because there is no information available about the elastic portion of a hardness test because no permanent impression is made until

the start of plastic deformation. In other words, to read a hardness number, there must be plastic deformation. Therefore, let us move on to an adjustable load situation where a hardness test is set up such that the test sequence starts with no load applied to the indenter and proceeds with an ever increasing load. Theoretically, in the very beginning, the metal under the ball would become more and more elastically distorted as the load increases until finally the load would reach a high enough level to overcome the elastic resistive forces of the metal. This load to indenter support area ratio would determine a hardness number that could be called a true elastic limit, and would be a measure of the start of plastic deformation. As was mentioned above, the problem in determining this measurement is that there is no information available except after the start of plastic deformation, i.e., at all loads up to the true elastic limit, the hardness numbers are infinite. Also, there is a bit of a problem in trying to interpret these very early stages of a hardness test because, in theory, the indenter touches the test material at a point, which would require a vanishingly small load to reach the true elastic limit. After the true elastic

limit is surpassed, the indentation process proceeds by plastic flow, and if the load were steadily increased, the indenter would keep sinking into the material until it reached the indenter diameter, beyond this condition the hardness number would be meaningless.

Situation (2): In a normal Brinell hardness test, the true elastic limit would be reached immediately and with no strain hardening, there would not be any further resistance to plastic deformation, i.e., the material under the indenter would be in a fully plastic state. Therefore, the indenter would sink into the material until a large enough indenter to material surface was produced to just support the applied load. This is a special situation and at least theoretically provides a method to measure a true elastic limit. This state would represent the load per support area where the material resistance to deformation is truly elastic without any strain hardening contributions. This hardness number (without strain hardening effects) would be lower than a normal hardness number where strain hardening is included.

Situation (3): At the very first moments of this test, the metal is again elastically deformed, and once again plastic deformation starts whenever the true elastic limit is reached, at this stage the material under the indenter becomes plastic (but not fully plastic) and the indenter moves into the test material. In contrast to situation (2), strain hardening takes place and the plastically deformed metal forms a resistance to continued plastic deformation that increases with the amount of plastic deformation. This results in a decreasing rate of descent of the indenter into the test material, and in fact, stops the indenter at some value short of the true elastic limit measurement of situation (2). This strain hardening resistance is a result of the plastic flow process, but appears as an increase in the elastic limit or an effective elastic limit of a plastically deformed metal. Thus, one might say that when the effective elastic limit has reached a high enough value, the indenter ceases to plastically deform the metal and a semi-equilibrium state is established where the load applied to the indenter is just balanced by the combined elastic resistances of the metal.

Another way to consider this type of hardness test is to evaluate the energy required or expended during the various processes. For instance, before the start of plastic deformation or up to the initial value of true elastic limit, all of the energy expended to distort the test material is recoverable. At the onset of plastic deformation, this is no longer the case. As soon as the indenter places a permanent indentation into the metal, energy is expended in one form or another. As plastic deformation proceeds, the amount of energy required to deform the material depends upon such factors as the amount of strain hardening, i.e., more strain hardening means more energy expended per unit of deformation or material volume displacement.

To put this analysis on a more quantitative basis and to include the effects of material properties as related to grain boundaries, the writer will attempt to explain these various processes with the aid of Figure 37, part a and part b. Figure 37, parts a and b, are graphs where Brinell Hardness Number has been plotted versus the dimensionless parameter d/D, where d is the

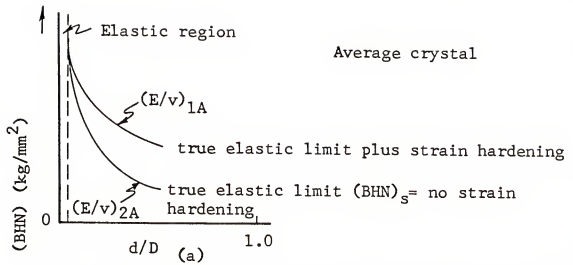

(a) Schematic representation of a Brinell Hardness Number versus a dimensionless parameter for an average crystal of 75-25 copper-zinc

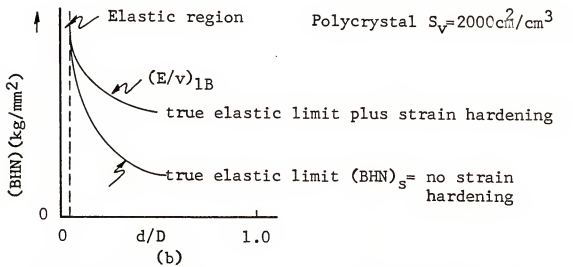

(b) Schematic representation of a Brinell Hardness Number versus a dimensionless parameter for a polycrystal (2000cm^2/cm^3) of 75-25 copper-zinc

Figure 37. Schematic representations showing the energy required to deform an average crystal and a polycrystal of 75-25 copper-zinc

chordal diameter of the hardness impression and D is the indenter diameter. Part a is for an average crystal of 75-25 copper-zinc while part b is for a polycrystal with S_v = 2,000 cm^2/cm^3. The energy per unit volume of deformation (E/v), shown on these graphs, refers to the measurements for Chattergee's (1956) analysis and are proportional to a Brinell Hardness Number.

The important points to be made with these graphs are: (1) $(E/v)_{1A} > (E/v)_{2A}$ for the average crystal, (2) $(E/v)_{1B} > (E/v)_{2B}$ for the polycrystal, (3) $(E/v)_{2A} \cong (E/v)_{2B}$ comparing the strainless hardness (BHN), for the average crystal polycrystal, and (4) $(E/v)_{1A} < (E/v)_{1B}$ comparing the average crystal and polycrystal.

It should also be mentioned that the elastic region shown would be infinitely small, but it was shown here to help in the interpretation.

APPENDIX V

GRAIN BOUNDARY DEFORMATION MODEL

Rhines (1965) introduced a model showing a sequence of events that characterizes the geometry of a grain boundary during plastic deformation. Following Rhines' (1965) explanation let us hypothetically form a grain boundary, look at its structure in relation to the conjoint grains, and sequentially follow a simple deformation process. To form a grain boundary, two grains that each have one perfectly clear randomly oriented flat surface are brought together along the flat surfaces and autogeneously welded. The weld interface could be called (1) a grain boundary, or (2) a crystallogrphic discontinuity within the bicrystal, i.e., the lattice planes in conjoint grains are not parallel. Supposing that no strains were introduced in the forming operation, what happens to the grain boundary interface during plastic deformation? For simplicity, bicrystal grains are now oriented such that slip planes in the separate grains are only different by simple tilt and twist angles, Figure 38, part a. The left hand grain is then plastically

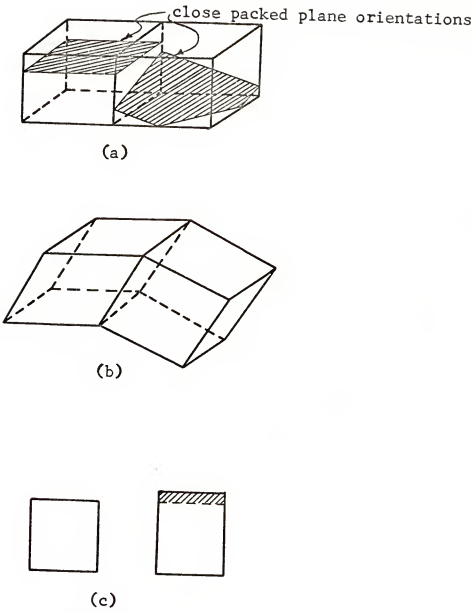

Figure 38. Schematic deformation of a bicrystal

deformed by a shearing operation, as is shown in Figure 38, part b. This plastic deformation necessarily deforms the grain boundary and since the right hand grain has been welded at the interface, it must conform to the shape change of the left hand grain. The right hand grain is not oriented correctly for simple accommodation at the grain boundary and therefore will necessarily deform along a different rotation path, Figure 38, part b. Thus by deforming the left hand grain, the right hand grain must also be deformed, but the right hand grain can only resist this deformation process along the grain boundary. Theoretically, if the grain boundary interface were removed from the bicrystal both before and after deformation, it would be found that the grain boundary area had increased during the plastic deformation process, Figure 38, part c. This increase in grain boundary area is a measure of a balance between:(1) the initial energy supplied to deform the left hand grain, and (2) the energy used up by the resistance of the right hand grain to deformation on a non-coincident set of slip planes under the continuity restrictions at the grain boundary. Thus, the increase

in grain boundary area is a direct measure of the amount of shear that has passed from the left hand grain to the right hand grain. It therefore follows, that the grain boundary deformation process can be characterized by the grain boundary area change during plastic deformation, without separately considering the dislocations, or the atomic interactions at the grain boundary interface.

Although this is a simple and rather presumptous example, the ideas formulated are germane to the understanding of a grain boundary's role in polycrystalline aggregate deformation.

APPENDIX VI

GRAIN BOUNDARY ENERGIES

It has long been known that intercrystalline and intracrystalline penetration of alpha brass by various solutions and liquid metals is sensitive to alloy composition. Since in general, liquid metal embrittlement along grain boundaries in alpha brass has been related to the relative liquid-to-metal and metal-to-metal surface energies, interest was generated in a comprehensive survey in recrystallized alpha brass. At the outset, it was assumed that a high grain boundary energy might also mean a high resistance of the grain boundary interface to plastic deformation.

Bates (1965) ran a set of experiments wherein he soaked seven different alloys of recrystallized alpha brass in liquid mercury for forty hours at $170 \pm 5^{\circ}C$. After the soaking operation, two different techniques were applied in an attempt to measure the liquid-to-solid dihedral angles along the grain boundaries. The first technique was to solidify the mercury in liquid nitrogen

and to section the specimens such that the bimetal interface was visible. After etching, an attempt was made to measure the root angles of the mercury penetrations along brass grain boundaries, but it was impossible. The smearing of the soft mercury precluded any clear definition of interfaces between the mercury and brass. As an estimate of penetration, the average depth of mercury penetration into the specimen along the grain boundaries was measured perpendicular to the brass specimen edge. The average depth of penetration, measured perpendicular to the brass-mercury surface is shown as a function of zinc concentration in Figure 39.

The second technique used was to evaporate the mercury from the brass specimens, mount the specimens, polish, etch, and then once again attempt to measure the root angles of the cracks that existed along the grain boundaries. The root angles were not clearly defined and could not be measured. Thus, once again estimates were made of penetration depth along grain boundaries perpendicular to the external brass surface, Figure 40, along

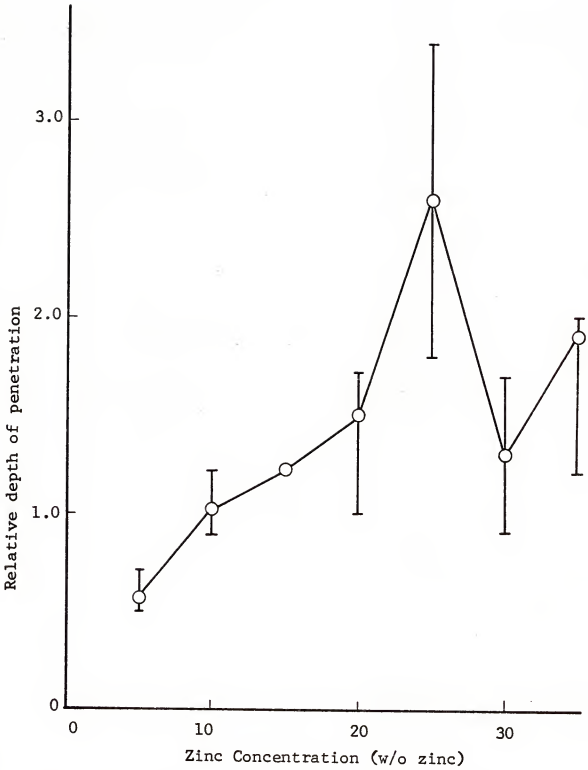

Figure 39. Average depth of penetration perpendicular to specimen edge versus zinc concentration in alpha brass with mercury still on the specimen

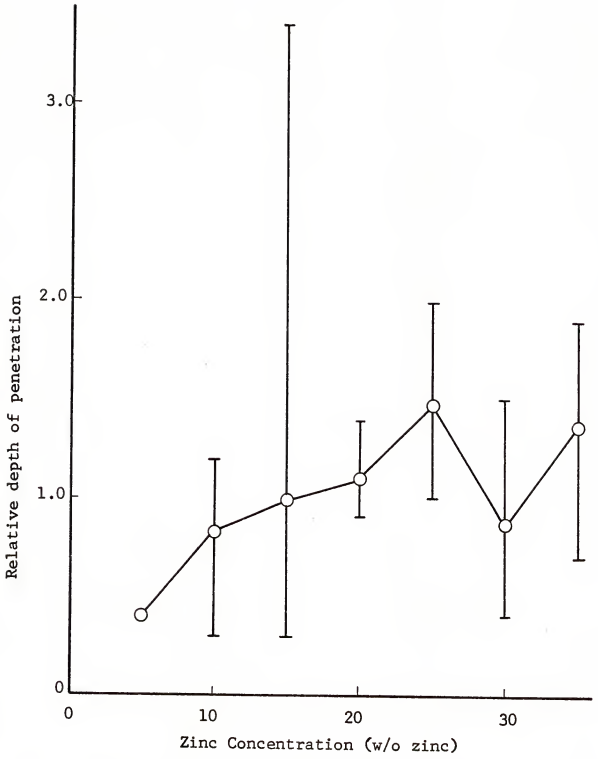

Figure 40. Average depth of penetration measured perpendicular to the specimen edge versus zinc concentration in alpha brass with mercury evaporated from the specimens

the path of the penetration, Figure 41, and also the average V-notch angle from the specimen surface to the bottom of the penetration, Figure 42.

Although the results look interesting, the measurements made were estimates and could only be used as an indication of the true dihedral angles.

The next attempt to measure true dihedral angle relationships of a liquid metal equilibrated along brass grain boundaries was made by the author. This was done by mixing approximately 3 w/o lead into molten alloys of alpha brass, cooling the ingots to room temperature, cold rolling and annealing to break up the cast structure, soaking the specimens at a temperature above the melting point of lead for several hours, and quenching. Supposedly, the lead globules along the brass grain boundaries equilibrate by the minimization of surface energies. Therefore, a measurement of the true dihedral angle between the liquid lead and solid brass can be used to estimate the relative energies of the liquid to solid interface and the grain boundary interfaces. This method, and the theory was explained by Smith (1948).

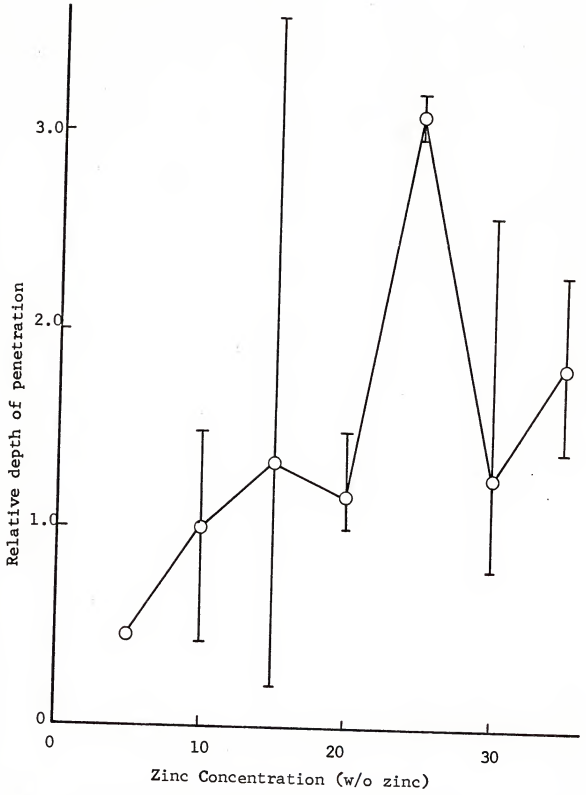

Figure 41. Average depth of penetration measured parallel to the penetration versus zinc concentration in alpha brass with the mercury evaporated from the specimens

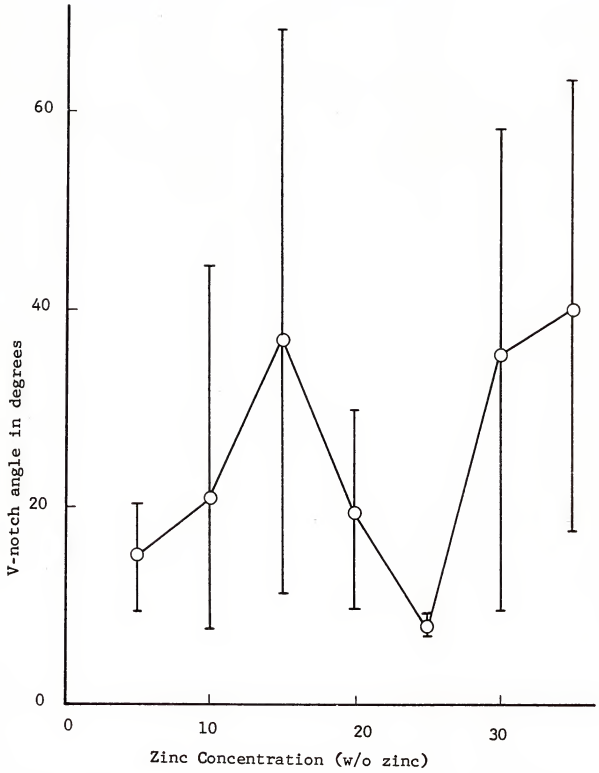

Figure 42. Average V-notch angle versus zinc concentration in alpha brass with the mercury evaporated from the specimens

The present experiments are broken down into two groups, group (1) is composed of four different brass alloys that were soaked at 450°C for 24 hours and quenched, while group (2) is composed of four specimens of the same alloy that were soaked at variable times and temperatures, followed by a quench. This information is summarized in Table XVI.

TABLE XVI

Alloy Compositions and Heat Treatments on Copper-Zinc-Lead Alloys

Specimen Number	Alloy Composition Cu - Zn - Pb	Heat Treatment time-temperature
1	87 - 10 - 3	24 hours @ 450°C
3	73 - 24 - 3	24 hours @ 450°C
4	63 - 34 - 3	24 hours @ 450°C
1A	93 - 4 - 3	84 hours @ 375°C
1B	93 - 4 - 3	60 hours @ 450°C
1C	93 - 4 - 3	24 hours @ 600°C
1D	93 - 4 - 3	12 hours @ 800°C

The frequency of dihedral angle versus dihedral angle graphs as measured on two-dimensional sections for specimens 1-4 are shown in Figure 43, parts a - d. A similar set of graphs for specimens 1A - 1D are shown in Figure 44, parts a - d.

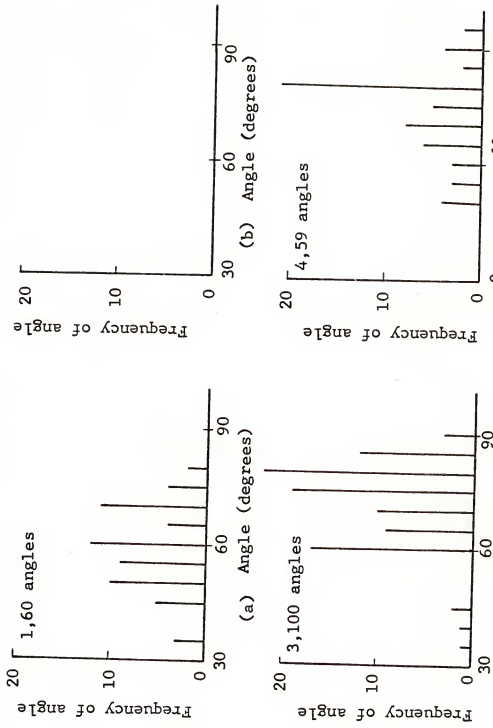

Figure 43. The angular distribution of dihedral angles in alpha brass

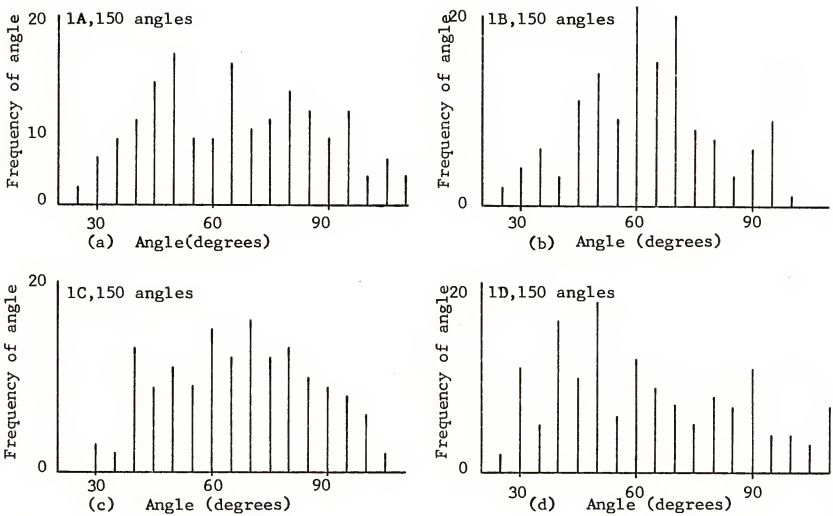

Figure 44. The angular distribution of dihedral angles for alpha brass

The reason that no information is given on specimen 2 is that it was accidentally destroyed during pretreatment.

APPENDIX VII

QUENCHING EXPERIMENTS

Quenching experiments will be summarized in three major groups according to composition: (1) 70-30, (2) 67-33, and (3) 65-35 copper-zinc.

Group (1): Two different sizes of specimens were quenched in attempting to "quench in" the high temperature material state. The first series used normal size hardness specimens that were quenched from 600°C into liquid nitrogen. The nitrogen was rapidly stirred during the quench, as were all quenching solutions. The hardness tests were made on the specimens within five minutes after the quench, and the tests were made with the specimens under the liquid nitrogen. The second series of 70-30 copper-zinc specimens were reduced in size to one-fourth of a normal hardness specimen, i.e., 0.25x0.25x1 inch, and quenched from 650°C into iced brine (266°K). These specimens were transferred to liquid nitrogen after a two-minute quench in iced brine, and were tested for hardness while under the liquid

nitrogen. The third series of specimens were also small and were quenched from 650°C into iced brine, but were warmed to room temperature before making hardness measurements.

The important result obtained from the first test series on 70-30 copper-zinc was that the normal boundary area contribution to hardness relationship was unchanged by quenching, Figure 45. No reason could be found to satisfactorily explain the low absolute values of the hardness numbers except possibly the specimens had not fully reached 77°K after quenching. These same specimens gave the normal room temperature hardness-boundary area relationship after warming the specimens to 298°K and testing immediately. The same hardness-boundary area relationship was also obtained when the specimens were again tested at room temperature after a time lapse of several months. The second and third series of experiments on small size 70-30 copper-zinc specimens was interesting but could not be used for comparisons because they were too small. The hardness test sampled the exterior (side) surfaces. The reason for including them was because the hardness-boundary area relationships were found to be

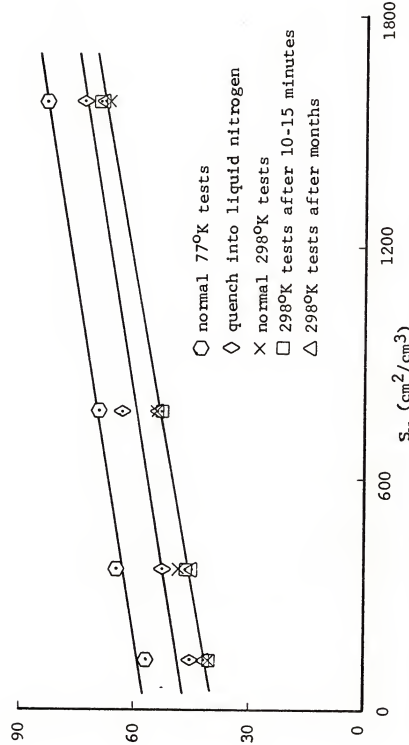

Figure 45. Brinell Hardness Number versus boundary area per unit volume relationships for the quenched, slow cooled and aged states of 70-30 copper-zinc

linear but low in magnitude and seemed to be a function of specimen size. This would imply that the exterior surface offers a unique resistance to plastic flow that is less than a grain boundary's resistance. The same boundary area plus external surface contribution to hardness was found at 77 and 298°K.

Group (2): The 67-33 copper-zinc alloys were prepared especially for the quenching experiments. The study on 67-33 copper-zinc was aimed at a comparison of: (1) furnace cooling, (2) slow cooling by natural means, and (3) quenching. This was done by: (1) allowing series of specimens to cool overnight in a furnace that was switched off at the end of the heat treating time, (2) removing another series from the furnace and allowing them to cool normally by standing in air at room temperature (the specimens were within a heat-treating chamber that also contained chips, and (3) quenching the third series into iced brine. The results of these experiments are shown in Figure 46 where hardness is plotted as a function of boundary area for all of the 67-33 copper-zinc specimens. The furnace-cooled and air-cooled specimens, shown by the

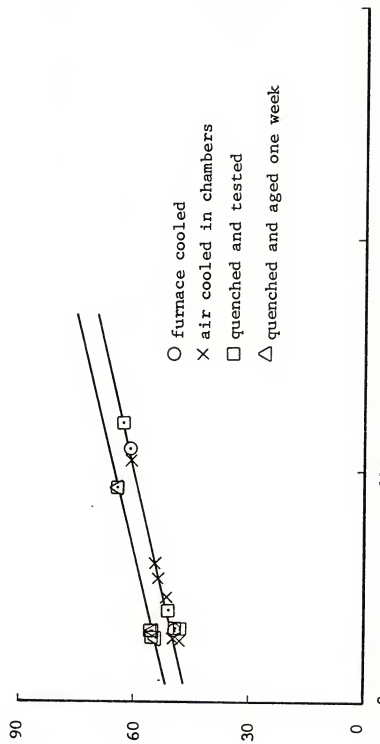

Figure 46. Brinell Hardness Number versus boundary area per unit volume relationships for the slow cooled, quenched and aged states of 67-33 copper-zinc

x's and circles respectively, give the same hardness versus boundary area relationships. The specimens that were tested for hardness immediately after quenching (the squares) and the hardness tests that were made after one week (the triangles) are also seen to give a similar boundary area contribution to hardness. The reason for the change in absolute magnitude of the hardness number with quenching is again unknown, but could be a result of quench strains induced by the specimen surface cooling faster than the specimen center.

Group (3): The last group of quenching experiments were on the 65-35 copper-zinc alloys. Several different boundary area specimens were quenched into iced brine from 600°C. The specimens were then immediately hardness tested at room temperature. This testing did not take more than two minutes from start to finish. The specimens were then allowed to stand at room temperature for one week, then the hardness was remeasured. The results of these tests are shown in Figure 47, where hardness is plotted versus boundary area. The squares represents the quenched state and the triangles represent the quenched and aged state.

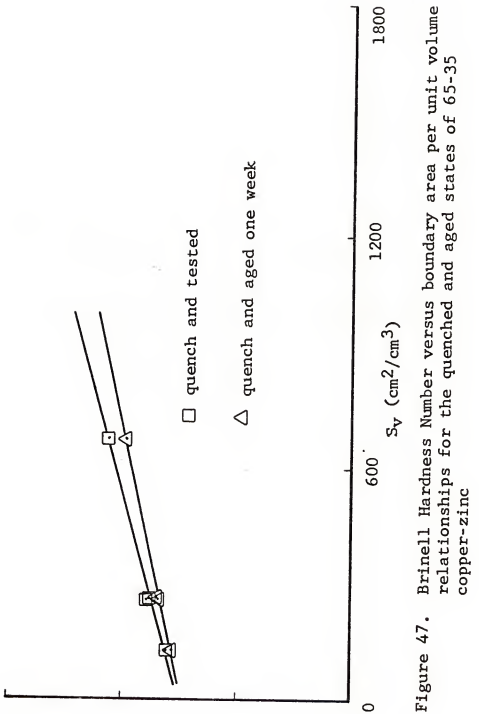

Figure 47. Brinell Hardness Number versus boundary area per unit volume relationships for the quenched and aged states of 65-35 copper-zinc

Note that the slope of the hardness-boundary area relationship has decreased with aging.

APPENDIX VIII

IMPURITY EFFECTS

"Equilibrium segregation" of impurities to grain boundaries is a widely accepted, but generally unproven phenomenon in metallic polycrystalline aggregates. The boundary area hardness contribution found in the present research could possibly fit an "equilibrium segregation" interpretation for explaining both composition and temperature dependencies. The importance of impurities was eliminated by the result that the same boundary area versus hardness relationships are obtained from different heats of the same composition brasses. To further check this effect, two series of 99.999 pure copper specimens were prepared such that each series covered about the same range of boundary area. The first series was prepared without any protection from the air. Internal oxidation of copper forms an oxide along the grain boundary interfaces, which would certainly act as an impurity. The second series of specimens were protected from oxidation. The hardness versus boundary area relationship for

both the oxidized and unoxidized copper are shown in Figure 48. The relationship is the same in the two cases.

Another check was made on impurity levels in all of the different brass alloys by making spectrographic comparisons with high purity copper and zinc. The spectrographic plate showed no anomalous lines.

Further analysis on the possibility of impurities was made by (1) making microprobe traces across grain boundaries at all compositions, and (2) making electron microscope replicas of the specimen surfaces at each composition. In both cases, the results were without unusual effects or anomalies.

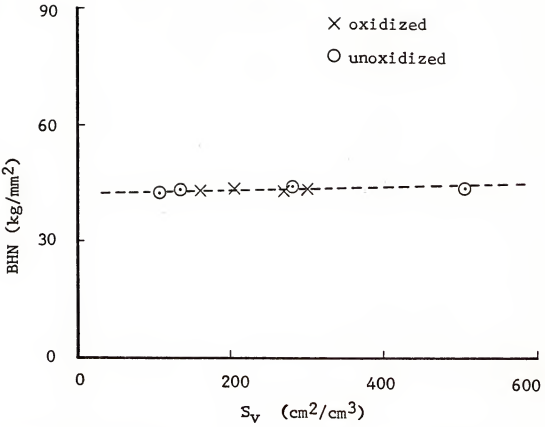

Figure 48. Hardness versus boundary area for oxidized and unoxidized specimens of pure copper

LIST OF REFERENCES

Adams, M.A., and Higgins, P.B., 1959, J.A.P., 30, 603.

Adams, M.A., Roberts, A.C., and Smallman, R.E., 1960, Acta. Met., 8, 329.

Angus, H.T., and Summers, R.F., 1925, JIM, 33, 115.

Argent, B.B., Blank, G., and Nissen, R., 1965, JIM, 93, 460.

Armstrong, R., Codd, I., Douthwaite, R.M., and Petch, N.J., 1962, Phil.Mag., 7, 45.

Atkins, A.G., Silvério, A., and Tabor, D., 1966, JIM, 94, 369.

Babyak, W.J. and Rhines, F.N., 1960, TAIME, 218, 21.

Baldwin, W.M., Jr., 1958, Acta. Met., 6, 139.

Bassett, W.H., and Davis, C.H., 1919, TAIME, 60, 428.

Bates, S., 1965, Senior Research, University of Florida.

Bell, W., Roser, W.R., and Thomas, G., 1964, Acta. Met., 12, 1247.

Bishop, J.F.W., and Hill, R., 1951, Phil. Mag., 42, 414, 1208.

Bragg, Sir L., 1942, Nature, 149, 511.

Chattergee, G.P., 1956, TAIME, 206, 454.

Churchman, A.T., 1960, JIM, 88, 221.

Clarebrough, L.M., Hargreaves, M.E., and Loretto, H.H., 1961, Proc. Roy. Soc., A261, 500.

LIST OF REFERENCES (Continued)

Codd, I., and Petch, N.J., 1960, Phil. Mag., 5, 30.

Conrad, H., 1961,"Electron Microscopy and Strength of Crystals," Interscience, N.Y., 299.

Conrad, H., 1963, Acta. Met, 11, 75.

Conrad, H., 1963, NPL Symp., HMSO, 244.

Conrad, H., and Christ, B., 1963, "Recovery and Recrystallization of Metals," Interscience, N.Y., 124.

Conrad, H., Feuerstein, S., and Rice, L., 1968, (to be published), J. Mat. Sci. and Engr.

Cottrell, A.H., 1953, Dislocations and Plastic Flow in Metals, (Oxford Press), 74.

Cracknell, A., and Petch, N.J., 1955, Acta. Met., 3, 186.

Desch, C.H., 1919, JIM, 2, 241.

Dingley, D.J., and McLean, D., 1967, Acta. Met., 885.

Duffin, R.J., Meussner, R.A., and Rhines, F.N., 1953, Carnegie Tech., Tech. Report No. 32, AF-33, 294.

Feltham, P., and Copley, G.J., 1959, Phil. Mag., 5, 649

Feltham, P., and Copley, G.J., 1960, Acta. Met., 8, 542.

Fisher, J.C., 1954, Acta. Met., 2, 9.

Flinn, P.A., 1960, TAIME, 218, 145.

Griffith, A.A., 1920, Phil. Trans. Roy. Soc., A221, 163.

Hall, E.O., 1951, Proc. Phys., Soc., B64, 747.

Harris, F.W., 1922, JIM, 28, 327.

LIST OF REFERENCES (Continued)

Heyn, 1903, The Metallographist, 6, 54.

Hill, R., 1952, Proc. Roy. Soc., 65A, 349.

Holloman, J.H., 1945, TAIME, 162, 268.

Hull, F.C., and Houk, W.J., 1953, TAIME, 197, 565.

Jeffries, Z., 1916, TAIME, 54, 594.

Jenkins, 1967, Senior Research, University of Florida.

Johnson, A.A., 1959, Phil. Mag., 4, 194; 1960, Acta. Met. 8, 737.

Keating, D.T., 1954, Acta. Met., 2, 885.

Kocks, U.F., 1958, Acta. Met., 6, 85.

Kocks, U.F., 1959, Acta. Met., 7, 131.

Kocks, U.F., 1967, private communication.

Köster, W., 1940, Z. Metall., 32, 160.

Köster, W., and Schüle, W., 1957, Z. Metall., 48, 589.

LeGris, 1911, Rev. Met., 8, 613.

Lemons, J.E., 1964, Masters Thesis, University of Florida.

Lips, E., and Sack, J., 1937, Nature, 8, 36; Z. Metall., 22.

Marcinkowski, M.J., and Fisher, R.M., 1965, TAIME, 233,233.

Meakin, J., and Petch, N.J., 1962, Symp. on the Role of Substructure, ASD-TDR-63-324-, 243.

Meyer, E., 1908, Z. des Vereines deutscher Ingenieure, 52, 645.

LIST OF REFERENCES (Continued)

Mohs, F., 1882, Grundriss der Minerologie, Dresden.

Mott, B.W., 1956,"Micro-Indentation Hardness Testing," (Butterworth Scientific Publications), 204.

Norbury, A.L., 1923, JIM, 29, 407.

Nowick, A.S., 1952, Phys.Rev., 88, 925.

O'Neill, H., 1934, The Hardness of Metals and Its Measurement (Chapman and Hall).

Petch, N.J., 1953, JISI, 174, 25.

Réaumur, 1722, L'Art de convertir le fer Forge en acier, Paris.

Rhines, F.N., 1965, Metallurgia-ABM, 21, 443.

Rhines, F.N., and Lemons, J.E., 1968, (to be published), TAIME.

Rhode, F., 1967, Senior Research, University of Florida.

Saltykov, S.A., 1945, Authors Certificate No. 72704, (USSR).

Sherby, O.D., 1962, Acta. Met., 10, 135.

Sherby, O.D., 1967, (to be published).

Shore, A.F., 1918, JISI, 2, 59.

Smith, C.S., 1948, TAIME, 175, 15.

Smith, C.S., and Guttman, L., 1953, TAIME, 197, 81.

Sorby, H.C., 1882, JISI, 21, 702.

Suzuki, H., 1965, J. Phys. Soc. Japan, 20, 1639.

LIST OF REFERENCES (Continued)

Swann, P.R., and Nutting, J., 1962, JIM, 90, 133.

Tabor, D., 1951, The Hardness of Metals (Oxford Press).

Takamura, J., and SeiMiura, 1959, J. Phys. Soc., Japan, 13, 1421.

Taylor, G.I., 1938, JIM, 62, 62.

Titel, R., 1953 (unpublished work referred to in Smith and Guttmann (1953)).

Thomas, G., 1963, J. Aust. Inst. Met., 8, 80.

Von Mises, R., 1928, Z. agnew. Math. u. Mech., 8, 161.

Wahlberg, A., 1901, JISI, 59, 243.

Westbrook, J.H., and Wood, D.L., 1963, JIM, 91, 174.

Wood, W.A., 1930, Phil. Mag., 10, 1073.

BIOGRAPHICAL SKETCH

Jack Eugene Lemons was born January 20, 1937, in St. Petersburg, Florida. He received his early schooling in Florida and was graduated from Tomlinson Vocational High School, St. Petersburg, Florida in 1955. For the next three years he was employed in heavy construction, surveying, and general machine shop work. In 1958 the author entered St. Petersburg Junior College and completed an Associates in Arts degree in June, 1960. The following September he entered the University of Florida, receiving a Bachelor of Metallurgical Engineering degree in 1963, a Masters of Science in 1964, and a Doctor of Philosophy in 1968.

The author is married to the former Benta M. Sorensen and has a son, Paul Eric. He is a member of AIME, ASM, ΣM and ΣX.

This dissertation was prepared under the direction of the chairman of the candidate's supervisory committee and has been approved by all members of that committee. It was submitted to the Dean of the College of Engineering and to the Graduate Council, and was approved as partial fulfillment of the requirements for the degree of Doctor of Philosophy.

June, 1968

Dean, College of Engineering

Dean, Graduate School

Supervisory Committee;

J. N. Rhinis
Chairman

R T D. Hall

James B. Conklin Jr. for J. Kronsbein

C. E. Reid